Global Biogeochemical Cycles

RESEARCH ARTICLE
10.1029/2021GB007286

Biological Carbon Pump Sequestration Efficiency in the North Atlantic: A Leaky or a Long-Term Sink?

Chelsey A. Baker[1], **Adrian P. Martin**[1], **Andrew Yool**[1], **and Ekaterina Popova**[1]

[1]National Oceanography Centre, Southampton, UK

Key Points:

- Lagrangian simulations show that North Atlantic Ocean sequestration efficiency of remineralized exported carbon (REC) varies strongly by region
- Only 66% of North Atlantic REC at 1,000 m will remain out of contact with the atmosphere for 100 years
- Fixed sequestration horizons ≤1,000 m can significantly overestimate long-term carbon sequestration

Supporting Information:

Supporting Information may be found in the online version of this article.

Correspondence to:

C. A. Baker,
chelsey.baker@noc.ac.uk

Citation:

Baker, C. A., Martin, A. P., Yool, A., & Popova, E. (2022). Biological carbon pump sequestration efficiency in the North Atlantic: A leaky or a long-term sink? *Global Biogeochemical Cycles*, *36*, e2021GB007286. https://doi.org/10.1029/2021GB007286

Received 17 DEC 2021
Accepted 28 APR 2022

Author Contributions:

Conceptualization: Chelsey A. Baker, Adrian P. Martin, Andrew Yool, Ekaterina Popova
Formal analysis: Chelsey A. Baker
Funding acquisition: Andrew Yool, Ekaterina Popova
Methodology: Chelsey A. Baker, Adrian P. Martin, Andrew Yool, Ekaterina Popova
Supervision: Adrian P. Martin, Andrew Yool, Ekaterina Popova
Visualization: Chelsey A. Baker
Writing – original draft: Chelsey A. Baker

Abstract The North Atlantic Ocean is a key region for carbon sequestration by the biological carbon pump (BCP). The quantity of organic carbon exported from the surface, the region and depth at which it is remineralized, and the subsequent timescale of ventilation (return of the remineralized carbon back into contact with the atmosphere), control the magnitude of BCP sequestration. Carbon stored in the ocean for >100 years is assumed to be sequestered for climate-relevant timescales. We apply Lagrangian tracking to an ocean circulation and marine biogeochemistry model to determine the fate of North Atlantic organic carbon export. Organic carbon assumed to undergo remineralization at each of three vertical horizons (500, 1,000, and 2,000 m) is tracked to determine how much remains out of contact with the atmosphere for 100 years. The fraction that remains below the mixed layer for 100 years is defined as the sequestration efficiency (SEff) of remineralized exported carbon. For exported carbon remineralized at the 500, 1,000 and 2,000 m horizons, the SEff is 28%, 66% and 94%, respectively. Calculating the amount of carbon sequestered using depths ≤1,000 m, and not accounting for downstream ventilation, overestimates 100-year carbon sequestration by at least 39%. This work has implications for the accuracy of future carbon sequestration estimates, which may be overstated, and for carbon management strategies (e.g., oceanic carbon dioxide removal and Blue Carbon schemes) that require long-term sequestration to be successful.

Plain Language Summary The North Atlantic Ocean is a key region for carbon uptake and organic carbon storage in the interior ocean for climate-relevant timescales (>100 years). Sinking organic carbon that reaches the interior ocean is respired there to form dissolved inorganic carbon. The fate of this carbon, that is, whether it remains in the ocean interior or returns to the surface and is ventilated to the atmosphere, depends on its physical circulation pathways. To investigate the efficiency of carbon storage in the North Atlantic Ocean we released virtual particles at three different starting depths (500, 1,000 and 2,000 m) into a global ocean model and tracked the pathways they followed for 100 years. 66% of virtual particles released at 1,000 m depth remained out of contact with the atmosphere for 100 years. Combining this pathway analysis with observation- and model-derived geographical fields of sinking carbon flux, we estimate that the 100-year North Atlantic carbon storage may be overestimated by 39% at 1,000 m because of this ventilation to the atmosphere. These findings have important implications for accurately estimating future ocean carbon storage. In particular, for carbon management strategies that require long-term sequestration to be successful (e.g., oceanic carbon dioxide removal and Blue Carbon schemes).

1. Introduction

Natural ocean carbon storage is driven by the biological carbon pump (BCP) via carbon export and the solubility pump via the subduction of dissolved inorganic carbon enriched waters (Volk & Hoffert, 1985). The BCP mediates the transfer of photosynthetically produced particulate organic matter from the surface ocean to the ocean interior via several pathways and pumps (Boyd et al., 2019). The depth to which particulate organic carbon (POC) penetrates is recognized as a key factor that determines the timescale that remineralized exported carbon (REC) will remain out of contact with the atmosphere. For example, it is generally assumed that POC that is remineralized in the mixed layer will likely exchange with the atmosphere in <1 year, POC that is exported below the mixed layer and into the upper mesopelagic (200–500 m) may be stored for decades, whilst POC that penetrates to the lower mesopelagic (500–1,000 m) and beyond may be stored on centennial timescales, depending on location (Antia et al., 1999; Lampitt et al., 2008; Robinson et al., 2014).

Oceanic carbon sequestration via the BCP is a crucial ecosystem system service as atmospheric CO_2 concentration is highly sensitive to the remineralization depth of exported carbon (Kwon et al., 2009). The economic value

Writing – review & editing: Chelsey A. Baker, Adrian P. Martin, Andrew Yool, Ekaterina Popova

of narrowing the uncertainty of the BCP carbon sequestration magnitude (CSM) was estimated to be ~US$500 billion based on a sequestration horizon of 500 m (Jin et al., 2020). This study highlights the wider implications and use of sequestration horizons, with the economic value of the BCP largely determined by the magnitude of the carbon sequestration estimates. Despite its considerable economic value, natural carbon sequestration via the BCP is often excluded from Blue Carbon assessments as it is not considered as a viable mechanism that can be managed to contribute to climate change mitigation (Lovelock & Duarte, 2019; Santos et al., 2021). However, an improved understanding of the fate of REC in the ocean is crucial for reliable predictions of the future ocean carbon sink, economic estimates of the value of BCP for policymakers and for nature-based solutions, such as ocean-based carbon dioxide removal (CDR), and Blue Carbon pathways that transfer organic carbon into the interior and deep ocean.

The North Atlantic Ocean is thought to be a key region for carbon sequestration via both the solublity pump, which delivers dense dissolved inorganic carbon-rich water to depth (Volk & Hoffert, 1985; Yashayaev & Clarke, 2008), and the BCP, which mediates the transfer of organic carbon export to the interior ocean (Lampitt et al., 2010; Lutz et al., 2002; Martin et al., 2011; Sanders et al., 2014). The Subpolar North Atlantic has important features for carbon sequestration such as the deep water formations regions at the start of the deep ocean conveyor (Yashayaev & Clarke, 2008) and the highly productive spring bloom (Martin et al., 2011). The low latitude North Atlantic also has features that may contribute to carbon sequestration such as upwelling along the North West coast of Africa which drives a localized region of high productivity (Helmke et al., 2005) and enhanced carbon sequestration in the oligotrophic gyre due to Saharan dust inputs (Pabortsava et al., 2017).

Carbon sequestration horizons are defined to estimate the magnitude of organic carbon stored in the ocean on climate-relevant timescales (100 years as used by the Intergovernmental Panel on Climate Change and other studies; Herzog et al., 2002; IPCC, 2007; Orr et al., 2001; Passow & Carlson, 2012). A widely used sequestration horizon, for both observation and model studies, is 1,000 m as carbon is typically thought to be stored for >100 years once it penetrates below that depth (Lampitt et al., 2008; Passow & Carlson, 2012; Robinson et al., 2014). However, assuming long-term sequestration at 1,000 m in the Southern Ocean overestimated the magnitude of potential carbon storage with only 33% of carbon sequestered for 100 years or more (71% at 2,000 m; Robinson et al., 2014). Other approaches to estimate the magnitude of long-term organic carbon sequestration are to use a fixed-density horizon at the top of the permanent pycnocline (1,027.6 kg m^{-3}; Guidi et al., 2015) or to estimate the sequestration efficiency (SEff) of regenerated nutrients using a data-constrained ocean circulation and biogeochemistry inverse model (DeVries et al., 2012). As noted by DeVries et al. (2012), the timescale until re-entrainment into the mixed layer depends on the location at which the export occurs and the depth at which organic carbon is remineralized, but fixed-depth sequestration horizons cannot on their own account for the downstream pathways and possible ventilation of REC.

The SEff and storage timescales of North Atlantic BCP carbon, estimated using nutrient inventories (DeVries et al., 2012; Weber et al., 2016), and for CDR schemes, or direct "injection" of CO_2 into the deep ocean (Siegel et al., 2021), have been explored using Ocean Circulation Inverse Models, which use static mean circulation and end of winter mixed layer depths (MLD; DeVries & Primeau, 2011). These studies find somewhat contrasting results in the North Atlantic, with DeVries et al. (2012) finding longer mean sequestration timescales compared to other ocean basins, whereas Siegel et al. (2021) found that the North Atlantic had shorter median (or mode) timescales relative to other ocean basins. These and other studies that explore BCP SEff and carbon sequestration often find differing spatial patterns, particularly in high latitude regions (DeVries et al., 2012; Guidi et al., 2015; Siegel et al., 2021; Weber et al., 2016). Further clarity on the role of ocean circulation for North Atlantic BCP carbon sequestration is needed and, in this study, we explore this further in a high-resolution global ocean model with temporally varying circulation and MLD, both of which can influence the downstream fate of REC.

Here we investigate the CSM and efficiency of BCP exported carbon in the North Atlantic Ocean guided by the IPCC's 100-year climate-relevant timescale and the widely used 1,000 m sequestration horizon (IPCC, 2007; Lampitt et al., 2008; Robinson et al., 2014). We use model simulations of Lagrangian particles, released at three sequestration depth horizons (500 m, 1,000 m and 2,000 m), to identify regions of high SEff as well as particle re-entrainment locations and timescales in the North Atlantic Ocean. We also assess how the choice of shallow and static depth sequestration horizons can impact the magnitude of carbon sequestration estimates, and explore the global implications for future ocean carbon sink predictions, economic estimates and Blue Carbon assessments, which are of global and societal importance.

2. Materials and Methods

2.1. Lagrangian Simulations

The long-term sequestration of BCP organic carbon is determined by the location and depth at which it is remineralized and the subsequent downstream pathway of the REC (DeVries et al., 2012). The downstream movement of REC is sometimes overlooked to simplify the approaches estimating carbon sequestration but it is a critical determinant of whether the carbon is stored on centennial, climate-relevant timescales. Here, we use a Lagrangian approach to explore the implications of the downstream pathways of REC to estimate the centennial magnitude and efficiency of carbon sequestration in the North Atlantic.

In this study we utilize Parcels (version 2.2.0; https://oceanparcels.org/; Delandmeter & Van Sebille, 2019; Lange & Van Sebille, 2017), an efficient, highly flexible, offline Lagrangian tool which tracks virtual particles, using the flow field of a hydrodynamic model, to undertake the Lagrangian particle-tracking simulations. Parcels enables Eulerian model fields to be extracted and outputted along particle trajectories. For these simulations we use 3D Runge-Kutta4 (RK4) timestep integration as the advection scheme, which uses an average of four approximations of the interpolated velocity field (which follows the mass conservation schemes of C grids) between successive timesteps to estimate the trajectory position (Delandmeter & Van Sebille, 2019; van Sebille et al., 2018). This has the advantage of reducing the magnitude of accumulated errors (van Sebille et al., 2018).

Simulations of Lagrangian particles were undertaken using Parcels which was applied to output from the Nucleus for European Modeling of the Ocean (NEMO) model, an ocean general circulation model (Madec, 2014). We utilized the NEMO model at 1/4° resolution, with greater resolution at high latitudes, and 75 vertical levels, with greater resolution in the surface ocean (ORCA025-N006). The ocean model was coupled to LIM2 a sea-ice model (Bouillon et al., 2009) and is forced with the historical atmospheric reanalysis Drakkar Forcing Set 5.2 (Brodeau et al., 2010). Surface boundary layer and interior vertical mixing in ORCA025-N006 NEMO were parameterized by a turbulent closure model (order 1.5; Blanke & Delecluse, 1993). The global ocean biogeochemistry was represented by MEDUSA-2, which is coupled with the NEMO model (Yool et al., 2013, 2015). The NEMO-MEDUSA simulation was restarted from 1990 NEMO output (which began in 1958) and ran from 1990 to 2015, but we excluded the first 6 years of the simulation in our analysis to allow the ocean biogeochemistry to adjust from the initial conditions. To approximate a 100-year simulation we cycled five times through 20 years of 5-day averaged circulation from 1996 to 2015.

The resulting 100-year velocity field was used to track water parcels via virtual Lagrangian particles released into the ocean circulation at three potential remineralization depths (500 m, 1,000 m and 2,000 m), which have been used as carbon sequestration horizons in prior studies (Guidi et al., 2015; Jin et al., 2020; Lampitt et al., 2008). A daily timestep was used for the RK4 timestep integration trajectory calculations, and a 5-day timestep was used for the trajectory output.

Lagrangian particles are used to track the flow of water parcels containing REC. We assume that for each Lagrangian particle release depth, the POC was completely remineralized into dissolved inorganic carbon at this depth, as in Robinson et al. (2014). These Lagrangian particles are tracking the physical trajectories only and do not represent sinking particles or quantities or concentrations of REC or POC.

Particles were seeded across an equidistant 60 km grid that accounts both for the curvature of the Earth and for submarine bathymetric features, the latter meaning that fewer particles were released deeper in the water column. For each sequestration horizon ~10,000 particles were released every month for 20 years (240 releases; 10,879 particles at 500 m, 10,453 at 1,000 m and 9,663 at 2,000 m). Particles were released at monthly intervals to ensure the conclusions of the study were not biased by release time. The trajectories of the 240 monthly releases were aggregated and ~2.3 million particles were analyzed to estimate the median 2-degree gridded sequestration metrics. We calculated a 2-degree gridded median to place the unevenly spaced data on a regular grid and to ensure a robust number of particles were used to calculate the sequestration metrics and to allow for comparisons to recent studies that present median timescales (Siegel et al., 2021).

We determine if a particle remains sequestered for the 100-year simulation by evaluating at every timestep whether each particle is deeper than the base of the local MLD field (as defined using a standard NEMO diagnostic of a 0.01 kg m^{-3} change in density with respect to that at 10 m; variable name ''mldr10_1''). This metric is based on the assumption that once dissolved carbon enters the mixed layer it is effectively in contact with the

atmosphere and will potentially outgas in <1 year (Antia et al., 1999; Jones et al., 2014; Palevsky & Doney, 2021; Quay et al., 2012). We compare the NEMO model 20 year mean and maximum MLD with an ARGO climatology, which includes two methodologies for calculating the MLD, termed the density threshold and the density algorithm (Holte et al., 2017). We aggregate all of the particle trajectories to determine what fraction of Lagrangian particles remain sequestered for the entirety of the 100-year simulation and use this to calculate the 2-degree gridded SEff. We define (SEff; %) as the percentage fraction of Lagrangian particles, representing REC, that remain sequestered for 100 years.

Previous Lagrangian studies have used a variety of MLD criteria to determine whether particles have been re-entrained, such as the model's local mean annual maximum MLD (Robinson et al., 2014), or an assumed, fixed MLD, such as 300 m to represent the Southern Ocean mixed layer (Drake et al., 2018). Our study takes a different approach and utilizes the instantaneous MLD along each particle trajectory to determine whether particles remain sequestered below the MLD or have been re-entrained into the mixed layer at each timestep. Once a particle has been re-entrained into the MLD, we exclude the remainder of the trajectory from our analysis.

At the time of running these experiments the parcels software was not adapted to allow particles to slip past coastlines or bathymetry (Delandmeter & Van Sebille, 2019), which can lead to particles beaching at the shoreline, or traveling across the bathymetric boundary, when using time-averaged velocity fields in conjunction with a Lagrangian timestep of 1 day. We chose a Lagrangian timestep of 1 day as a computational trade off between the model output frequency (5 day means) and the length of our simulation (100 years). As our analysis was dependent on particles either being re-entrained into the mixed layer or reaching the end of the simulation we could not include beached or ''out of bounds'' particles. To reduce the instances of particles crossing a bathymetric boundary we add a criterion that returned particles to 10 m above the seafloor if they crossed a topographic boundary, which reduced the fraction of out of bounds particles. A small number of particles at each release depth were continually moved across the seafloor boundary due to strong vertical downwelling currents (1.76%–3.56%) or were beached around islands with rapidly shoaling topography (0.16%–1.16%). These particles were not analyzed as part of this study.

2.2. Organic Carbon Flux and Sequestration

The magnitude of organic carbon storage estimates can vary greatly depending on the depth of the chosen sequestration horizon, as it is often assumed that ventilation from these depths is negligible on 100-year timescales. Here, we refer to carbon sequestration as the storage of carbon in the ocean for climate-relevant timescales, defined as a minimum of 100 years, guided by the timescales assessed by the Intergovernmental Panel for Climate Change (IPCC, 2007). In this study, we combine 6 satellite-derived estimates (see Section 2.2.2) and the MEDUSA model downward carbon fluxes with our Lagrangian analysis to calculate the North Atlantic CSM at each particle release depth and location, and to calculate an integrated estimate of the centennial CSM (TgC yr^{-1}) for the North Atlantic.

2.2.1. Model Organic Carbon Fluxes

Organic fast- and slow-sinking carbon fluxes at 500 and 1,000 m are standard NEMO-MEDUSA output (Yool et al., 2013) and were extracted from the ORCA025 NEMO-MEDUSA simulation used to provide the velocity fields for the parcels simulations. Organic carbon fluxes at 2,000 m are not standard MEDUSA model output. To estimate the organic sinking carbon flux at 2,000 m we calculated Martin's b (Martin et al., 1987) for each water column between the total flux at 1,000 m and the total detrital flux at the seafloor by rearranging Equation 1 (Boyd & Trull, 2007). Equation 1 uses Martin's b to predict a particle flux profile based on a power-law model and a b value of −0.858 has been widely used in literature (Martin et al., 1987). F_{z0} is the flux at shallower reference depth $z0$ and F_z is the flux at depth z (Equation 1). Once Martin's b had been estimated for each water column we used Equation 1 to predict the flux at 2,000 m (F_z) using the flux at 1,000 m as F_{z0}. Martin's b provides an upper bound estimate of fluxes due to the nature of the power-law and is known to be sensitive to the chosen export depth (Cael & Bisson, 2018). To ensure the choice of attenuation profile would not bias our results we also estimated the 2,000 m fluxes by calculating the remineralization length scale (RLS) for each water column and depth-corrected the 1,000 m fluxes using an exponential model (Equation 2; Cael & Bisson, 2018) which is used in the MEDUSA biogeochemical model to parameterize attenuation of fast-sinking carbon fluxes (Yool

et al., 2013). However, the results were very similar and so we only present the power-law model which uses estimates of b to depth-correct the fluxes in this study.

$$F_z = F_{z0} \cdot (z/z0)^{-b} \quad (1)$$

$$F_z = F_{z0} e^{-(z-z0)/\mathrm{RLS}} \quad (2)$$

2.2.2. Satellite-Derived Organic Carbon Fluxes

To expand our results beyond the MEDUSA biogeochemical model we have also estimated carbon fluxes using satellite observations. Organic carbon fluxes at 500 m, 1,000 m and 2,000 m were estimated from satellite-derived net primary production (NPP) coupled with algorithms for export and attenuation. NPP products use chlorophyll *a*, photosynthetically active radiation (PAR) and sea surface temperature (SST) observations. To ensure the estimated flux magnitudes were not biased by the algorithms and empirical relationships we use combinations of two standard primary production data products, two empirical models of export production at 100m, and two empirical models of the attenuation of this exported material with depth leading to six different observation-derived carbon flux estimates.

NPP was estimated using the Vertically Generalized Production Model (VGPM; Behrenfeld & Falkowski, 1997) and the Carr (2002) algorithm. The VGPM NPP 2003–2019 monthly estimates were downloaded directly from http://sites.science.oregonstate.edu/ocean.productivity/index.php. The MODIS chlorophyll *a,* PAR and SST monthly products used to estimate the VGPM NPP were downloaded and also used with the Carr algorithm to estimate NPP. Clouds in the MODIS data were filled using the VGPM gap-filling algorithm.

Export production at 100 m was estimated by multiplying VGPM NPP and Carr NPP by the *pe*-ratio of Dunne et al. (2007) and the ThE_i ratio of Henson et al. (2011) to create four estimates of export at 100 m. The Dunne et al. (2007) algorithm is based on particle export ratio observations between 0.04 and 0.72 and hence any calculated ratios in this study that were below 0.04 were set to the lower bound and above 0.72 were set to the upper bound, as in Henson et al. (2011).

Particle fluxes at 500 m, 1,000 m and 2,000 m were estimated using export estimates (where $z0 = 100$ m) and the Martin equation with a b value of −0.858 (Martin et al., 1987, Equation 1). Particle fluxes were also estimated using the Lutz et al. (2007) algorithms which use NPP and the seasonal variation index of NPP. We present and compare the patterns of the satellite derived fluxes in Text S2 and Figures S2—S7 in Supporting Information S1.

2.2.3. Carbon Sequestration Magnitude

The downward carbon fluxes at 500 m, 1,000 m and 2,000 m from the MEDUSA model and the satellite-derived fluxes were multiplied by the grid area. The fluxes were re-gridded to same 2° regular grid as the sequestration metrics and SEff and summed to estimate the annual North Atlantic CSM. The gridded spatial maps of the fluxes were scaled using the spatial maps of SEff (%)

$$\mathrm{CSM}_{100\mathrm{yr}} \left(\mathrm{TgCyr}^{-1}\right) = \mathrm{CSM} \times (\mathrm{SEff}/100) \quad (3)$$

to estimate the annual magnitude of BCP carbon that remains sequestered on centennial timescales ($\mathrm{CSM}_{100\mathrm{yr}}$). The estimates are summed to calculate the magnitude of centennial carbon sequestration in the North Atlantic and the percentage decrease due to re-entrainment of REC is presented.

3. North Atlantic Carbon Sequestration Pathways and Efficiency

3.1. Sequestration Metrics

The fraction of Lagrangian particles, representing REC, that are re-entrained into the mixed layer depends on the depth and location at which the Lagrangian particles are released (i.e., the remineralization location and depth), and the subsequent downstream pathway, with re-entrainment driven by the seasonal and latitudinal variation in MLD along the particle trajectories (Figure 1). The NEMO model mean and maximum MLD compares well to the ARGO climatology but the MLDs penetrate too deep in the Labrador Sea, which is a known issue in NEMO models (Figure 1; MacGilchrist et al., 2021; Marzocchi et al., 2021).

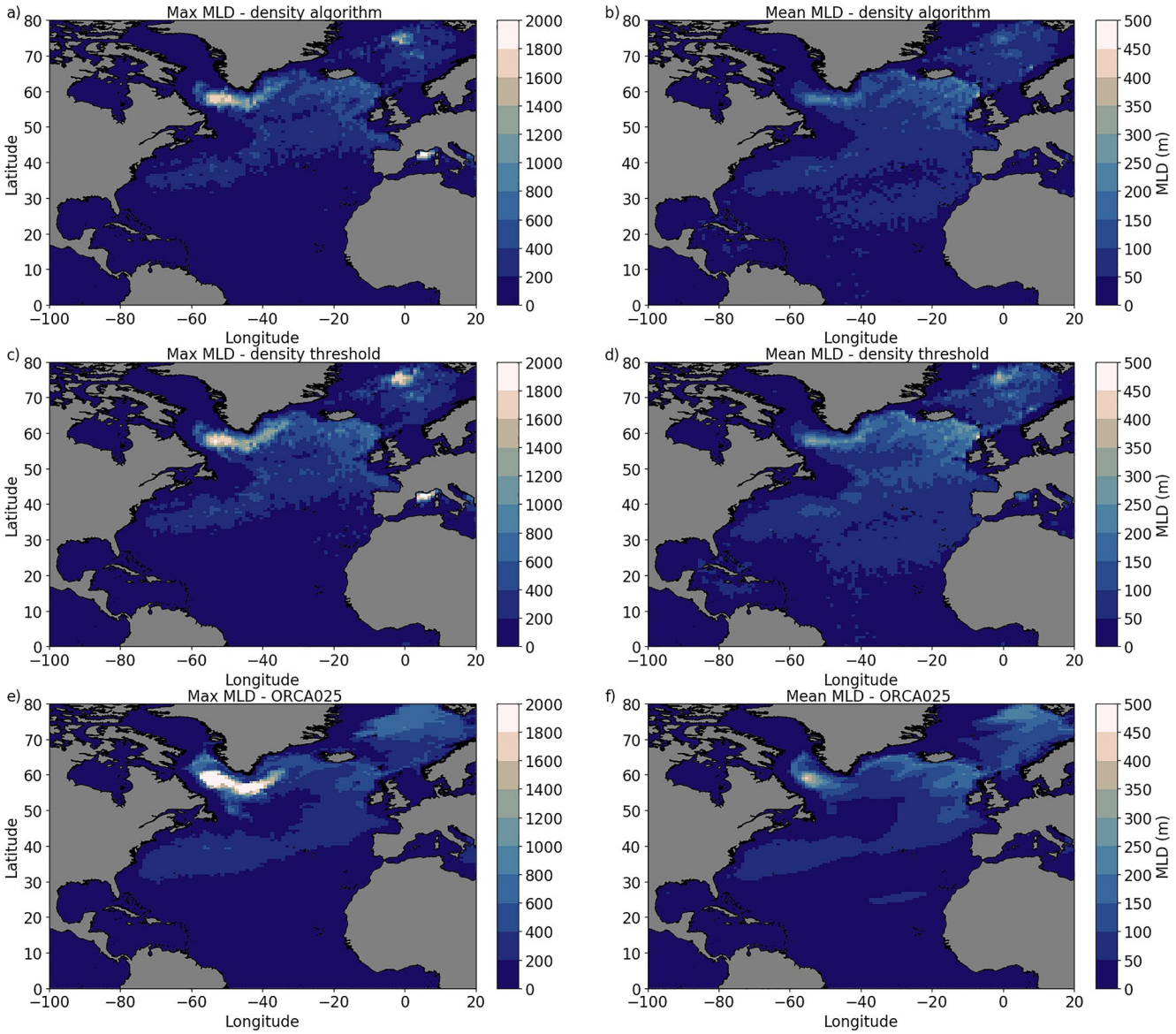

Figure 1. North Atlantic maximum and mean mixed layer depths (MLD) calculated from ARGO monthly composites of the maximum (a), (c) and mean MLD (b), (d), respectively (Holte et al., 2017) and Nucleus for European Modeling of the Ocean (ORCA025) model 20 year maximum (e) and mean (f) of monthly average MLD. The density threshold and density algorithm estimates of MLD from Holte et al. (2017) are presented.

Of the 240 (12 months × 20 years) North Atlantic Lagrangian particle releases at 500 m, 1,000 m and 2,000 m, 71.8%, 34.2% and 6.5% of particles respectively were re-entrained into the mixed layer and were not sequestered (Table 1). Therefore, 28.2%, 65.8% and 93.5% of Lagrangian particles respectively, representing REC, released at 500 m, 1,000 m and 2,000 m, were sequestered for a minimum of 100 years, implying long-term sequestration in the interior ocean. The release time of the particles had a negligible impact on the statistics of the sequestration metrics, both in terms of monthly or seasonal variability, and was not explored further in this study (Table S1 in Supporting Information S1).

Of the North Atlantic Lagrangian particle releases at 500 m, 1,000 m and 2,000 m, re-entrained particles took 16.9, 32.0 and 48.6 years (median timescale), respectively, to reach the base of the mixed layer (Table 1). The median time until particle re-entrainment increased as the release depth increased (Table 1 and Figure 2).

There are several areas of interest in Figures 2 and 3 and we explore the spatial differences of the timing and depth of re-entrainment here. The median time until re-entrainment is <5 years for the central Labrador Sea for

Table 1
A Summary of the Fate of Lagrangian Particles Released at Three Different Sequestration Horizon Depths in the North Atlantic Ocean

Sequestration horizon (Particle release depth; m)	Re-entrained particles (%; +/− std)	Sequestration efficiency (Sequestered particles; %)	Median re-entrainment time (Years from start)
500	71.8 (±0.54)	28.2	16.9
1,000	34.2 (±0.48)	65.8	32.0
2,000	6.5 (±0.43)	93.5	48.6

Note. The mean (± standard deviation; std) percentage of re-entrained and sequestered particles (SEff; the sequestration efficiency), and the median time until re-entrainment is presented for each release depth for all of the successfully released particles.

the 2,000 m releases and this area of rapid re-entrainment expands as release depth shoals, with the majority of the Labrador Sea, Subpolar North Atlantic and the Greenland, Iceland and Norwegian seas particles re-entrained within 5 years for the 500 m particle releases (Figure 2). This is due to deep winter mixed layers in the Subpolar North Atlantic and the fast-moving current pathway that traverses along the bathymetry of the Iceland Basin, joins the Irminger current and skirts the Labrador Sea (Marzocchi et al., 2015; Pickart et al., 2002; Yashayaev & Clarke, 2008).

In contrast, Lagrangian particles released in the Eastern (sub)tropical North Atlantic remain below the mixed layer for much longer timescales before re-entrainment (Figure 2) and fewer particles are re-entrained (Figure S2 in Supporting Information S1). The region in the vicinity of the Northwest African upwelling, extending from the coast of Senegal to Liberia, had no particles released at 2,000 m subsequently re-entrained into the mixed layer, suggesting it is a highly efficient region for long-term sequestration (Figure 2f; greyed out ocean area). This is further supported by the median depth and particle density of sequestered particles at the end of the simulation in Figure 4, with a much greater density of sequestered particles found in the Eastern subtropical North Atlantic.

As expected, the deeper the release depth of the Lagrangian particles the greater the depth of re-entrainment, and particles persisted below the base of the mixed layer for longer timescales (Table 1). The Labrador Sea was

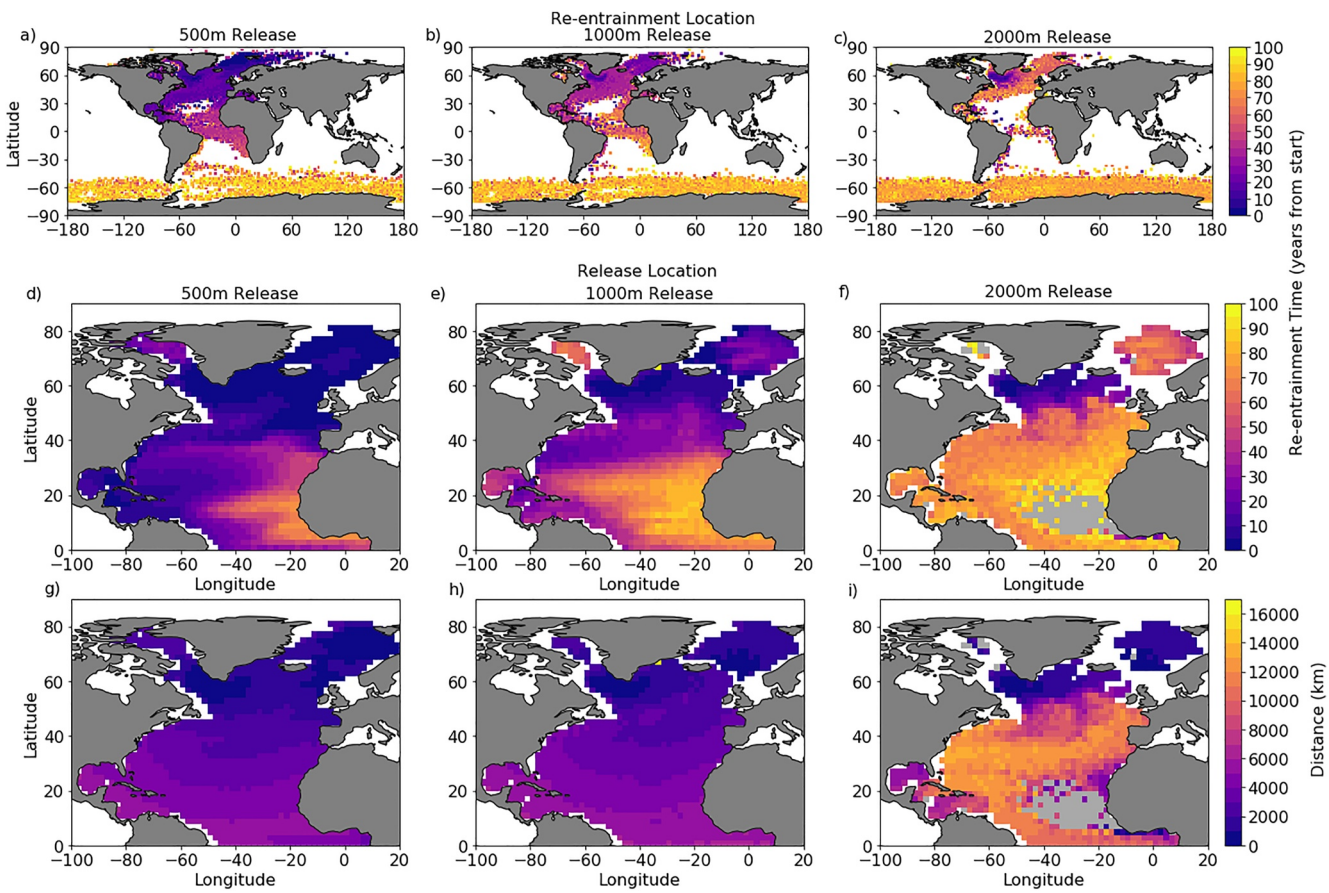

Figure 2. The timing of Lagrangian particle re-entrainment into the mixed layer shown at the re-entrainment location (a, b and c) and release location (d, e and f). The release to re-entrainment distance (linear, not along trajectory; g, h and i) for the three release depths 500 m, 1,000 m and 2,000 m. Light gray shaded grid cells in the North Atlantic Ocean (f, i) indicate that none of the Lagrangian particles released from that location were re-entrained into the mixed layer within the 100-year simulation.

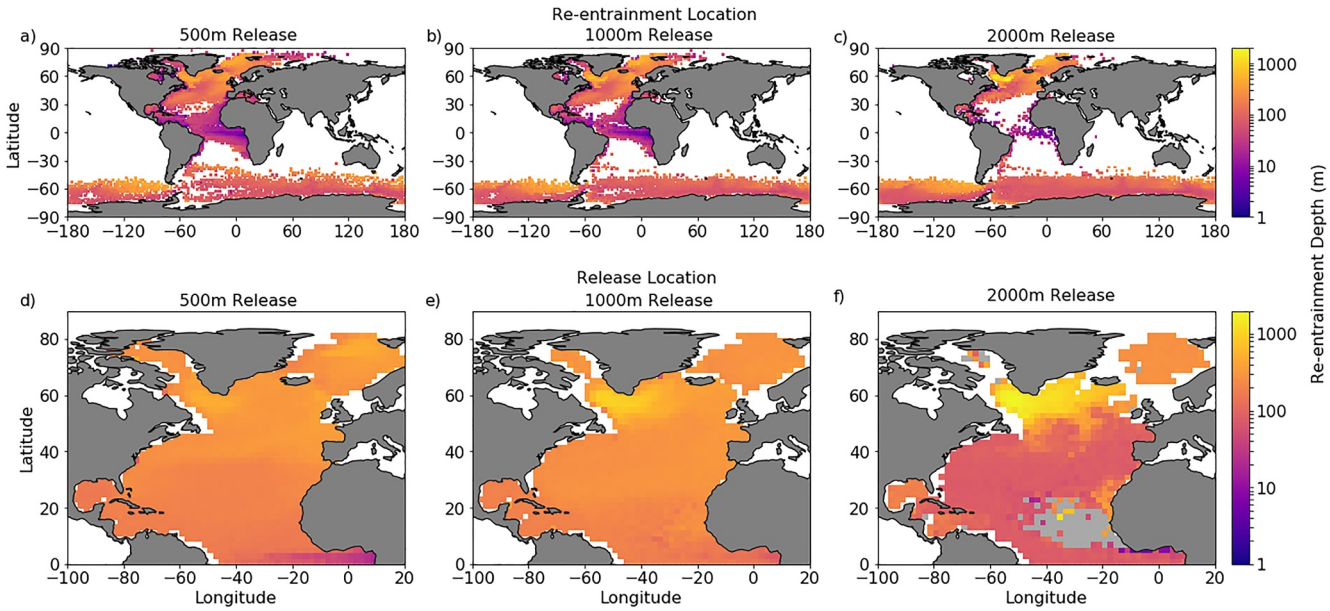

Figure 3. Median re-entrainment depth of Lagrangian particles shown at the location of re-entrainment into the mixed layer (a, b and c) and shown by the release location of re-entrained particles (d, e and f) for the three release depths 500 m (a), (d), 1,000 m (b), (e) and 2,000 m (c), (f). Light gray shaded grid cells in the North Atlantic Ocean (f) indicate that none of the particles released from that location were re-entrained into the mixed layer within the 100-year simulation.

the most prominent ventilation point, due to the deepest winter MLDs (Figures 1 and 3). The Subpolar North Atlantic and the Greenland, Iceland and Norwegian seas were also prominent regions of re-entrainment due to deep winter mixed layers. The Labrador Sea had the highest density of re-entrained particles for the 1,000 m and 2,000 m particle releases, whereas the Greenland-Iceland-Faroes shelf region, the Subpolar North Atlantic and the Gulf stream were all important regions for particle re-entrainment for the 500 m particle releases (Figure S2 in Supporting Information S1). Other regions of particle re-entrainment into the mixed layer were the North Atlantic current, the Gulf of Mexico, the Caribbean Sea, the North Atlantic equatorial region and the Southern Ocean (Figures 2 and 3 and S2 in Supporting Information S1). For all regions, except the Southern Ocean, the number of particles being re-entrained in these regions decreased with release depth (Figure S2 in Supporting Information S1). 35.3% of re-entrained particles released at 2,000 m were re-entrained into the mixed layer in the Southern Ocean (35-90S), compared to only 0.2% and 1.5% for the 500 and 1,000 m releases. Particles released at 2,000 m traverse different pathways compared to the shallower releases, with a major pathway, likely North Atlantic Deep Water (NADW; 2,000 m particles were released at potential densities between 1,027.73 and 1,028.09 kg m^{-3}, with a mean density of 1,027.86 kg m^{-3}, consistent with upper NADW water mass definitions 1,027.85–1,028.10 kg m^{-3}; Liu & Tanhua, 2021), which flows along the Western Atlantic and into the Southern Ocean, where REC may be upwelled (Figures 2 and 3). This different behavior is supported by the greater distances traveled by re-entrained Lagrangian particles released at 2,000 m in Figure 2i, compared to subplots 2g and 2h, and the shallower re-entrainment depth between 0 and 50N in Figure 3f, compared to subplots 3d and 3e.

Particles that remain sequestered throughout the 100 year simulation tend to remain at depths similar or deeper than the release depth, except for particles South of 55S, which tend to be shallower (<600m) in the water column at the end of the 100 years simulation (Figures 4a, 4c and 4e) but they are small in number compared to those that remain within the Atlantic (Figures 4b, 4d and 4e). This may suggest that the latter would have become re-entrained into the Southern Ocean mixed layer (~300m) within 10s of years if the simulation was extended beyond 100 years. However, some sequestered particles that pass through the South Atlantic are entrained into deep water masses (>2,500 m) between ~30 and 55S and spread into the deep Pacific and Indian Oceans, which are likely to have long residence times (100s yrs; Siegel et al., 2021), and this pathway is particularly prominent in the 2,000 m simulations (Figure 4).

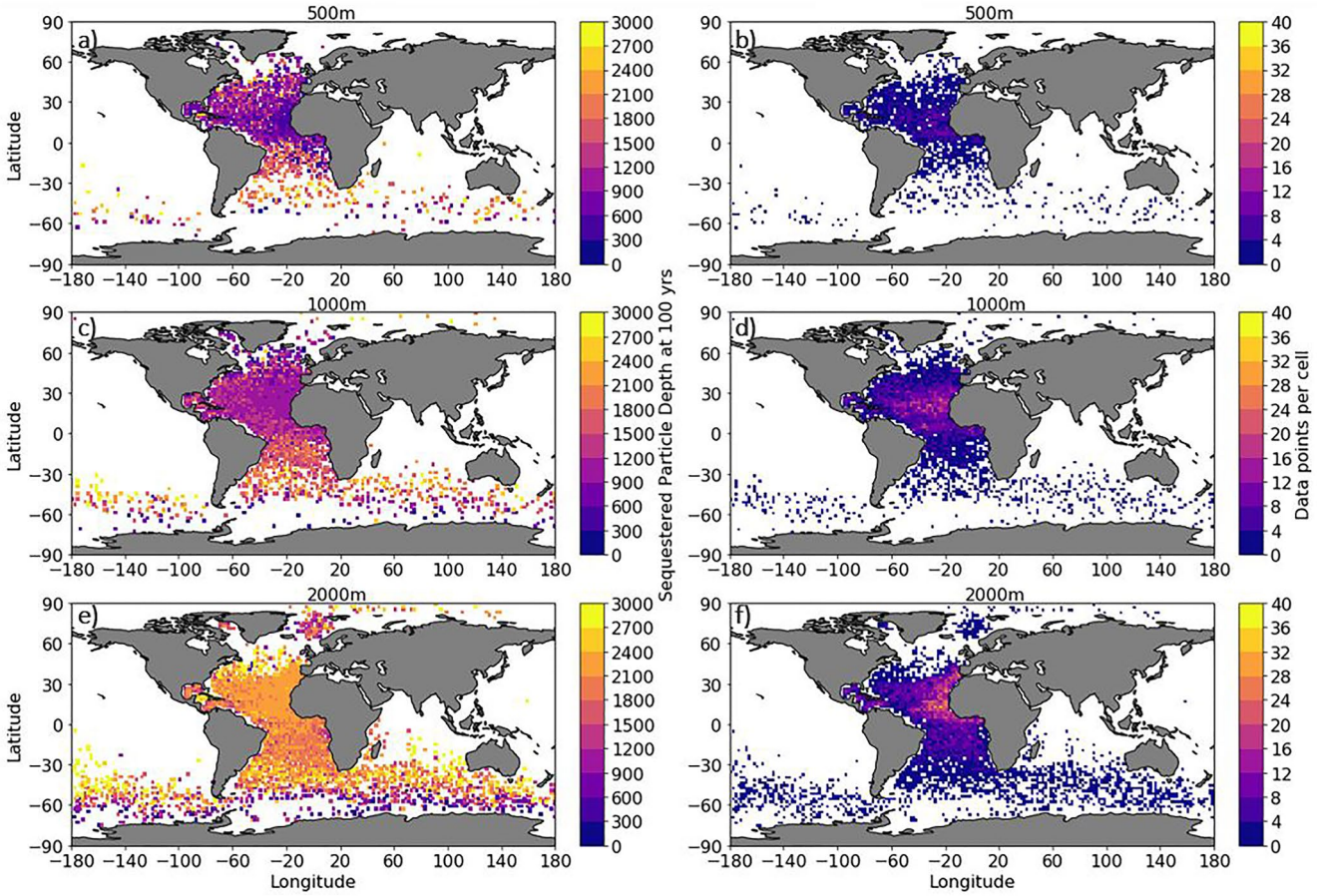

Figure 4. An example of the location and median depth of sequestered Lagrangian particles for each 2 × 2° gridded water column 100 years after the first particle release at (a) 500 m, (c) 1,000 m and (e) 2,000 m. The density of data per 2 × 2° water column is shown for the (b) 500 m, (d) 1,000 m and (f) 2,000 m particle releases.

3.2. North Atlantic Carbon Sequestration Magnitude

As expected, the SEff, calculated by determining the fraction of Lagrangian particles that remained below the mixed layer for the 100-year simulation, was greater for particles released deeper in the water column (Figures 5a–5c). The regions of greater sequestration efficiencies were the Eastern (sub) tropical North Atlantic (extending further North and West for the deeper release depths) and the band extending from the Gulf stream and Grand Banks across to the Eastern North Atlantic (Figure 5). As the released particles represent REC this provides an estimate of the fraction of carbon that would remain sequestered for 100 years once remineralized at 500 m, 1,000 m or 2,000 m.

Organic carbon fluxes between 500 and 2,000 m have been used in the literature (Guidi et al., 2015; Henson et al., 2012; Jin et al., 2020) to estimate the magnitude of global or regional long-term sequestration. The results of this study indicate that not all of the organic carbon flux that reaches these depths will remain out of contact with the atmosphere. To estimate the magnitude and patterns of the carbon sequestration fluxes, we used both the MEDUSA organic carbon flux and the six different satellite-derived carbon flux estimates at each sequestration horizon (CSM_{100yr}; see Text S2 and Figures S2—S7 in Supporting Information S1). The values presented are lower limit estimates as the SEff scaling assumes that all carbon at each depth horizon is remineralized instantaneously, whereas a proportion of that flux will typically be transferred deeper into the ocean interior.

The spatial pattern of 100-year sequestered carbon (CSM_{100yr}; Figures 5g–5i) is similar for the three release depths, with more localized regions of greater carbon fluxes at 500 m compared to wider coverage but lower carbon flux magnitudes at 2,000 m. The key regions for long term storage are the Subpolar North Atlantic (excluding deep winter mixing regions in the Labrador Sea and the Irminger Sea), the Gulf Stream and North

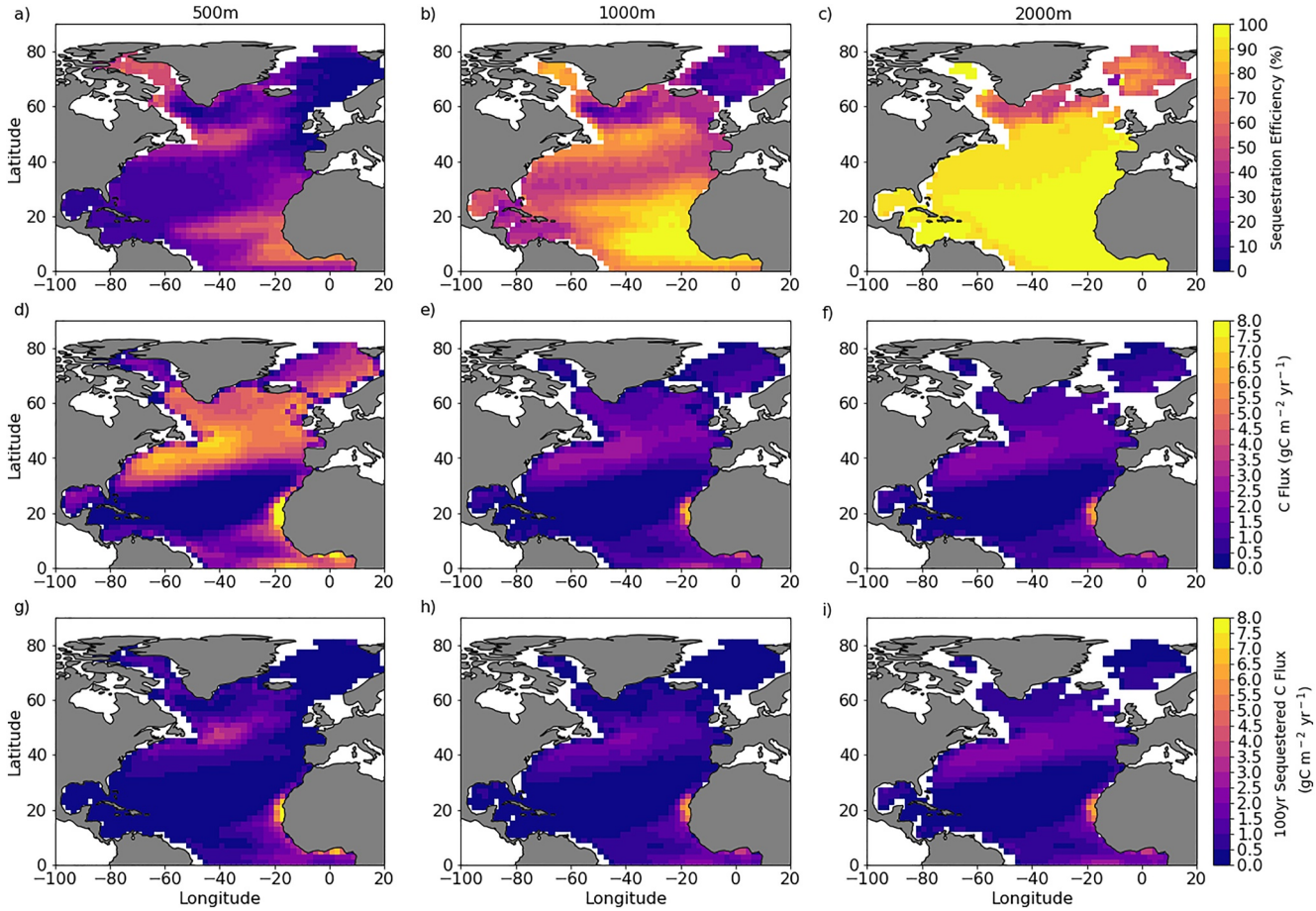

Figure 5. Sequestration efficiency of the Lagrangian particles representing remineralized exported carbon during the 100-year experiment at 500 m (a), 1,000 m (b), and 2,000 m (c). Organic carbon fluxes from the MEDUSA biogeochemical model (d, e, f; gC m^{-2} yr^{-1}) and carbon fluxes scaled using the centennial sequestration efficiency, termed 100 years sequestered carbon, CSM_{100yr} (g, h, I; gC m^{-2} yr^{-1}). Note the different colorbar scales.

Atlantic current region, and the Eastern (sub) tropical North Atlantic. The spatial pattern of sequestered carbon fluxes at 2,000 m is very similar to the original carbon flux driven by generally high SEff at 2,000 m in the North Atlantic.

To estimate the cumulative impact of the subsequent re-entrainment of REC within 100 years on North Atlantic carbon storage estimates we calculate the total downward carbon fluxes for the MEDUSA model of 107.7, 39.2 and 33.2 TgC yr^{-1} at 500 m, 1,000 m, and 2,000 m (Figure 6). We then combine each flux estimate with the gridded SEff independently at each depth horizon to scale the fluxes to estimate the REC that will avoid re-entrainment within 100 years (Equation 3). For the MEDUSA carbon storage estimates this leads to similar annual CSM_{100yr} of 28.9, 24.8 and 30.4 TgC yr^{-1} at 500 m, 1,000 m and 2,000 m respectively, which is a decrease of 73.2%, 36.7% and 8.3%. These results emerge due to the balance between carbon flux attenuation, which leads to lower carbon fluxes deeper in the water column, and SEff, which increases with depth. As the CSM_{100yr} is estimated using the spatial maps of carbon fluxes and SEff, there are regions where CSM_{100yr} at 1,000 m is greater than at 500 m, with increases in SEff compensating for lower carbon fluxes. This is shown for some estimates in Figure 6 where bold orange bars (1,000 m) are larger than the bold red bars (500 m). It appears that, to first order, the attenuation of carbon fluxes (for both model and observational estimates) and ventilation timescale cancels out, demonstrated by the annual CSM_{100yr} estimates being of a similar magnitude at the three depth horizons.

To ensure our conclusions are not biased by the spatial pattern or magnitude of carbon fluxes in the MEDUSA model we also compared 6 different combinations of satellite NPP, export and flux algorithms (see Figures S2—S7 and Text S2 in Supporting Information S1). The mean total downward carbon fluxes for the satellite estimates are 178.6, 95.0 and 42.5 TgC yr^{-1} at 500 m, 1,000 m and 2,000 m (Figure 6) whereas when accounting

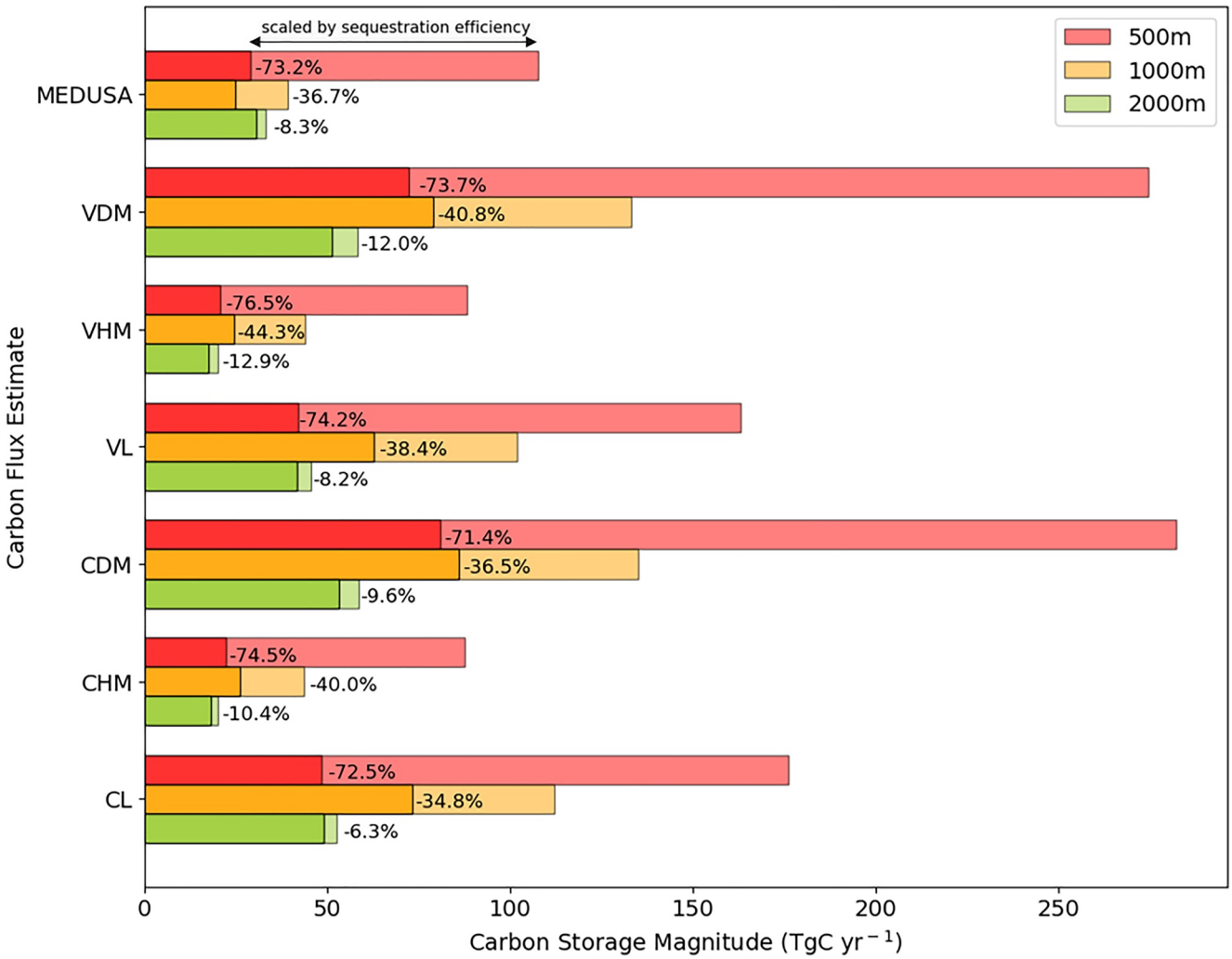

Figure 6. Carbon Storage Magnitude (TgC yr^{-1}) derived from organic carbon fluxes at each sequestration horizon (500 m – red, 1,000 m – orange, 2,000 m – green) from the MEDUSA biogeochemical model and satellite-derived estimates (V = VGPM, C = Carr, D = Dunne, H = Henson, M = Martin, L = Lutz). The fluxes at each depth (faded colors) have been scaled using the gridded SEff independently at each sequestration depth horizon (Figures 5a–5c) to demonstrate the magnitude of carbon that would subsequently be re-entrained within 100 years (CSM_{100yr} – bold colors).

for subsequent re-entrainment of REC the sequestration magnitude decreases to 47.7, 58.5 and 38.4 TgC yr^{-1} at 500 m, 1,000 m and 2,000 m. The satellite estimates exhibit a mean percentage decrease of 73.8%, 39.1% and 9.9% at 500 m, 1,000 m and 2,000 m respectively (Figure 6), which is very similar to the MEDUSA percentage decreases. This indicates that the spatial pattern and magnitude of the downward carbon fluxes from observations and the MEDUSA model are similar (Figures 5 and 6 and Figures S2—S7 in Supporting Information S1).

From our estimates the magnitude of CSM_{100yr} in the North Atlantic ranges between 17.3 and 85.8 TgC yr^{-1} (Figure 6 – bold bars) but on average is broadly similar at 500 m, 1,000 m and 2,000 m with a magnitude of 41.3 ± 26.9 PgC yr^{-1}. This demonstrates how shallow carbon sequestration horizons (≤1,000 m) can considerably overestimate CSM when assuming that none of the REC will be ventilated within 100 years. Furthermore, the spatial patterns of SEff in Figures 5a, 5b, 5c highlight that using static depth horizons may also over/underestimate carbon sequestration depending on the region but our results show that the cumulative effect is an overstated magnitude of carbon sequestration for the North Atlantic. This highlights that the magnitude of flux, the flux location and remineralization depth are key to determining the timescales that REC remains out of contact with the atmosphere, as the location and depth determines the downstream pathway of REC.

4. Discussion

4.1. North Atlantic Ocean Sequestration Efficiency

The North Atlantic Ocean is typically viewed as a key region for carbon sequestration via the biological pump, due to the pulse of export associated with the spring bloom, which can efficiently transfer organic carbon to the interior ocean (Briggs et al., 2011; Martin et al., 2011). North Atlantic deep water formation regions are also thought to be important for natural carbon sequestration, as REC in these regions can follow deep pathways at the start of the thermohaline circulation, leading to long sequestration timescales (Bower et al., 2019; Yashayaev & Clarke, 2008). Our results indicate that high export and deep water formation regions which are typically associated with these key processes are not necessarily the only areas of importance for long-term organic carbon sequestration. The source region of REC, in terms of location and depth, will determine its downstream pathway, which appears to be a crucial determinant of SEff. In this section we first discuss the source regions with high sequestration efficiencies and then discuss key pathways and re-entrainment regions.

Our results demonstrate that the greatest magnitude of carbon sequestered for 100 years is within and adjacent to a region off the Northwest coast of Africa which has both continuous (20°–33°N) and seasonal (12°–20°N) upwelling, with the majority of upwelled waters originating along the continental slope between 100 and 300 m (Marcello et al., 2011; Mittelstaedt, 1983, 1991). Initially, it appears counterintuitive that interior water masses in the vicinity of, or even beneath, an upwelling region would have a high CSM. However, the region has high productivity, leading to comparatively high carbon fluxes, and with upwelling waters originating from depths shallower than 300 m (which tend to extend only ∼50 km away from the shelf break; Mittelstaedt, 1983), it is possible for a significant fraction of remineralization to occur below the soon-to-be-ventilated waters. Downstream pathways of particles released at 500 m and below do not appear to interact with regions of upwelling waters but instead interact with the subtropical gyre shadow zone in the eastern tropical North Atlantic characterized by weak circulation (Kounta et al., 2018; Luyten et al., 1983). Therefore, the region in the vicinity of the Northwest African upwelling is a highly efficient area for long-term sequestration via the BCP (Figure 5).

Another region of widespread carbon sequestration is the North Atlantic Current region, extending from North of the Gulf stream up to Iceland, and, when using 1,000 m and 2,000 m sequestration horizons, extending across to the Eastern Atlantic (Figure 5). In particular, the region adjacent to Grand Banks off Newfoundland is a hotspot at the shallowest particle release depth, with moderate sequestration efficiencies and large annual downward carbon fluxes. This region also stood out as an efficient region for carbon sequestration in the satellite-derived CSM_{100yr} estimates (Figures S2—S7 in Supporting Information S1), with the areas of higher carbon storage and the relative importance of the Grand Banks adjacent region compared to the North West African upwelling region varied between the estimates.

The regions of highest or lowest SEff determined by our Lagrangian approach (Figure 5 and Section 3.2) have been identified in other global studies. However, in some regions the opposite trend was reported. For example, the Labrador Sea was determined to be a high SEff region (DeVries et al., 2012) rather than a region of low SEff as found here. Typically, a low-resolution (2° horizontal resolution), data-constrained inverse circulation model, which utilizes temporally fixed fields, is used to determine spatial variability of SEff (DeVries & Primeau, 2011; Siegel et al., 2021). Previous studies have specifically focused on regenerated nutrients (DeVries et al., 2012) or deep ocean nutrient inventories as a tracer of particulate organic matter remineralization (Weber et al., 2016). Regions of deep mixing were found to be efficient for long-term carbon sequestration in an inverse model which evaluated regenerated nutrients with a mean sequestration timescale for North Atlantic regenerated organic matter of 150–400 years (DeVries et al., 2012). However, inverse models evaluating deep ocean nutrient inventories or injected CO_2 found shorter sequestration timescales and similar regions of high efficiency (regions adjacent to Grand Banks and North African upwelling) and low efficiency (Gulf stream and North Atlantic current) with the exception of the Labrador Sea which varies between studies (Siegel et al., 2021; Weber et al., 2016). The differences in the results may be due to the different approaches (i.e., inverse models vs. Lagrangian particle-tracking) and tracers used (regenerated vs. deep ocean nutrients). Furthermore, differences in model resolution, which has implications for the circulation and the range of MLDs (i.e., 2° for inverse models vs. 0.25° NEMO-MEDUSA model), or in the nature of the circulation state used (i.e., a static vs. time-varying flow field) may also lead to the differences in the spatial patterns but exploring the details of these is beyond the scope of this study.

High latitude regions with deep winter MLDs, such as the Labrador Sea, are the regions with the least agreement between different methods. This is likely due to differences in MLD climatologies, for example, low resolution (2° horizontal resolution) Ocean Circulation Inverse Models calculate MLD from annual mean potential temperature and salinity from World Ocean Atlas (DeVries et al., 2012; DeVries & Primeau, 2011) or use an ARGO MLD climatology (de Boyer Montégut et al., 2004; Devries, 2014) whereas our study uses local, temporally variable model MLDs. However, it should be noted that ocean models have difficulty reproducing and agreeing on areas of deep convection, especially at low resolution, as was demonstrated by Heuzé (2017) for CMIP5 models. Finally, the assumptions of the methodology, including the role of the MLD used to estimate the long-term sequestration, will further drive differences between the studies. For example, in DeVries et al. (2012) the high sequestration efficiencies and long sequestration timescales observed in the Labrador and Greenland, Iceland and Norwegian seas are attributed to the global pattern of ocean circulation as these are the regions where deep and bottom waters form. However, there is evidence from previous model and Lagrangian studies that interannual variability in winter MLD (Macgilchrist et al., 2021), mesoscale eddies (Georgiou et al., 2020) and the subsequent re-entrainment of NADW in the Southern Ocean (Tamsitt et al., 2017) may impact the long-term sequestration of REC in this region. These aspects may not be captured using low-resolution inverse models, such as the Ocean Circulation Inverse Models used in DeVries et al. (2012), which may overstate the importance of the Labrador Sea in long-term sequestration of REC.

Additionally, our Lagrangian simulation results found that particles released in the central Labrador Sea often take <5 years to be re-entrained into the MLD (Figure 3). A previous MITGCM model study found that the export of dense water masses takes >6 years in the central Labrador Sea and is mediated by eddy activity via entrainment into the fast-moving boundary current (Georgiou et al., 2020). The 0.25-degree NEMO model used to force our Lagrangian simulations has a similar fast-moving boundary current skirting the Labrador Sea (Marzocchi et al., 2015), but is only eddy-permitting. It is possible that the REC in Labrador Sea interior water masses may be re-entrained into the mixed layer in the NEMO model (Georgiou et al., 2020; MacGilchrist et al., 2021), instead of entering the deep limb of the NADW. This supports our finding that the Labrador Sea is a highly inefficient region for organic carbon sequestration.

The Lagrangian experiments revealed a major pathway from the North Atlantic to the Southern Ocean, which had particular importance for Lagrangian particle releases at 2,000 m. The pathway from the North Atlantic to the Southern Ocean is an important route for re-entrainment into the mixed layer (Figure 2), because of the circumpolar wind-driven upwelling that takes place there, but carbon that passes through the Southern Ocean can also be sequestered for >100 years in deep water masses (Figure 4). Particles re-entrained in the Southern Ocean are a small fraction of the re-entrained particles from the 500 and 1,000 m releases (0.2% and 1.5%), with a re-entrainment time of 85.0 and 82.6 years, respectively (median timescale; bracketed by the 100-year simulation length), but make up a considerable fraction of particles re-entrained from the 2,000 m releases (35.3%) with a re-entrainment time of 77.3 years. NADW is found below 1,500 m in the North Atlantic and flows out of the Atlantic into the Southern Ocean, where it has later been found to upwell (Tamsitt et al., 2017). This aligns well with our 2,000 m particle release results (Figures 2 and 3) and with the NADW water mass density range which overlaps with the density of the Lagrangian particles released in some regions at 2,000 m.

A previous Lagrangian study investigating SEff in the Southern Ocean found that, for a sequestration depth of 1,000 m, 66% of the carbon was re-exposed to the atmosphere within 100 years, taking an average of 38 years to do so, while, for a depth of 2,000 m, only 29% of the carbon was re-exposed within 100 years, taking an average time of 58.4 years (Robinson et al., 2014). This suggests that on 100-year timescales the North Atlantic may be more efficient for carbon sequestration than the Southern Ocean.

We cannot determine from this study how long North Atlantic REC that enters the Southern Ocean will remain sequestered beyond the 100-year simulation. Heatmaps of the sequestered trajectory depths at 100 years for the three release depths (Figure 4) indicate that there are deep ocean (>2,000 m) pathways that particles traverse within and out of the Southern Ocean. For Lagrangian particles releases at 500 m, 1,000 m and 2,000 m, 2.0%, 2.0% and 6.6% of sequestered particles respectively, had passed out of the Atlantic Ocean (crossed 45S) into the Indian, Pacific or Southern Oceans within 100 years and were deeper than 2,000 m at the end of the simulation. This implies that these particles may remain out of contact with the atmosphere for longer timescales than 100 years. This is supported by a study investigating the global sequestration timescales of CDR in which

the Pacific and Indian Oceans were identified as efficient pathways for long-term carbon sequestration (Siegel et al., 2021).

Two processes we do not explicitly consider in this study are the timescale of mixing from the base of the mixed layer to the ocean surface and the timescales of air-sea gas exchange. Air-sea gas exchange is not instantaneous but we assume that once REC enters the mixed layer it will remain there long enough to re-equilibrate with the atmosphere (Ito & Follows, 2013; Siegel et al., 2021). However, as the equilibration timescale of carbon dioxide is between 6 and 18 months, this means that subduction of partially equilibrated waters could allow for a greater SEff of REC than we have estimated here (Jones et al., 2014). In particular, regions with deep winter mixed layers may also have longer gas exchange timescales (Jones et al., 2014), but we cannot assess this with our approach.

4.2. Sequestration Horizons Overstate Carbon Storage

We have evaluated the SEff of BCP carbon reaching three depth horizons using a high-resolution Lagrangian methodology. Our results have demonstrated that using carbon sequestration horizons of a static depth, which do not account for spatial variability in the subsequent movement of REC, overestimate the magnitude of long-term carbon storage in the ocean compared to the CSM_{100yr} estimates we present that account for ventilation. In particular, the static depth horizons overestimate storage magnitude in deep mixing regions, such as in the Subpolar North Atlantic, while potentially underestimating the long-term storage magnitude in regions that are highly efficient at sequestering carbon for 100 years at shallower depths, such as the Eastern (sub)tropical Atlantic. The net effect for the North Atlantic is to overestimate the CSM as shown by Figure 6, for both model and observation-derived carbon fluxes. Whilst this study focuses on the North Atlantic, it is likely that fixed sequestration horizons of 1,000 m or less that are applied globally also overestimate the magnitude of carbon storage, particularly for regions upstream of deep MLDs.

Using fixed sequestration horizons ≤1,000 m may be appropriate for some localized regions but may lead to large overestimates of CSM if applied over entire basins. SEff estimated from Lagrangian particles released at 2,000 m was >90% for the majority of the North Atlantic, but using deeper sequestration horizons will lead to more conservative estimates of sequestration and will overlook a fraction of REC that was remineralized shallower in the water column. One previous approach used the base of the permanent pycnocline (except in deep winter mixed layer regions) as a spatially variable carbon sequestration horizon, producing a larger estimate for global organic carbon sequestration (0.72 PgC yr^{-1} vs. 0.33 PgC yr^{-1}) compared to using a fixed 2,000 m horizon (Guidi et al., 2015). The density criterion was replaced in deep MLD regions with the annual mean MLD calculated from the seasonal maximum MLD in each cell from the de Boyer Montégut et al. (2004) climatology (Guidi et al., 2015). More recent ARGO MLD climatologies, with a much greater number of profiles and improved methods of determining the MLD, generally have deeper winter MLDs in the Subpolar North Atlantic than the de Boyer Montégut et al. (2004) climatology, with MLDs extending down to 1,800 m in the central Labrador Sea (Holte et al., 2017). Therefore, the seasonal maximum MLD climatology used in Guidi et al. (2015) may have been considerably shallower in deep mixing regions compared to the winter maximum MLD, which may have inflated estimates of carbon sequestration in regions, such as the Labrador Sea, compared to our estimates which are derived using the local temporally varying MLD.

Using the depth of the permanent pycnocline as a sequestration horizon (Guidi et al., 2015) may be too conservative (>1,000 m) in regions such as the (sub) tropical Eastern Atlantic, as in this study, we show that at 500 and 1,000 m a considerable magnitude of carbon can be sequestered at these depths in the Eastern Atlantic (Figures 5g and 5h). The depth of the permanent pycnocline may be a useful approach (Guidi et al., 2015), with an improved representation of the sequestration horizon in deep mixing regions, for evaluating carbon sequestration over longer timescales (i.e., average ocean turnover time of 1,000 years; Primeau, 2005) but is likely to underestimate the magnitude of carbon sequestered on centennial timescales.

The estimates of CSM_{100yr} combines the SEff and the downward carbon fluxes and therefore depends on the magnitude of carbon fluxes at different depths and how this varies spatially. The carbon fluxes will be affected by various assumptions about the shape of the attenuation profile for the MEDUSA model and the satellite-derived carbon fluxes. The MEDUSA model organic carbon fluxes are composed of two sinking detrital pools, fast-sinking (implicitly represented) and slow-sinking (explicitly represented; Yool et al., 2013). Slow-sinking detrital material can be advected within the model, which means that the slow-sinking contribution to total carbon fluxes

may have been advected away from the initial export location. However, the contribution of slow-sinking detritus to the total annual carbon flux is small (<12% at 500 m and <2% at 1,000 m). A power law model (Equation 1) was used to to depth-correct the 1,000 m MEDUSA model fluxes to estimate the flux at 2,000 m and to predict the attenuation of export at 100m for 4 of the satellite-derived flux estimates. Whilst the choice of export depth and assumptions about the shape of the attenuation profile can impact the magnitude of carbon fluxes, the differences were negligible when depth-correcting model carbon fluxes and comparing the power law model (upper bound; Equation 1) to an exponential model (lower bound; Equation 2, Cael & Bisson, 2018). Furthermore, the satellite-derived fluxes that use the Lutz empirical model fell in the middle of the other estimates and demonstrated similar values of CSM_{100yr}, suggesting that the results are not sensitive to the choice of attenuation profile at the depths presented here (Lutz et al., 2007).

It is challenging to determine how future estimates of carbon sequestration may change as this will depend on the cumulative effect of changes in SEff driven by physical changes and changes in carbon export by the BCP due to biogeochemical changes. Under future climate change, the oceans are predicted to become increasingly stratified, meaning shallower MLD and reduced nutrient supply and the overturning circulation is predicted to become more sluggish (DeVries et al., 2017; Steinacher et al., 2010). These predicted physical changes may enhance the SEff of future REC but nutrient trapping in the deep ocean may reduce the magnitude of exported carbon via the BCP (Bopp et al., 2001). The spatial pattern of these two climate driven changes may lead to compensating effects for future long-term sequestration of BCP exported carbon, with implications for the magnitude of the ocean carbon sink in the future and for organic carbon that has already been exported to the deep ocean.

4.3. Is There a Local Proxy for Sequestration Efficiency?

We explored whether a proxy of the SEff determined in this study could be found using ''local'' model properties such as maximum MLD. A SEff proxy would expand our capabilities to evaluate future predictions of BCP sequestration by the current generation of Earth System Models (ESM). ESM simulations at present are run at low resolution (usually 1°) meaning Lagrangian simulations would not produce accurate trajectories due to the simplified physics of the models, that is, implicit subgrid scale parameterizations of small-scale circulation features (Gent & Mcwilliams, 1990; Madec, 2014), which means that advection would not represent the full flow field. Without a proxy for SEff comparisons between different models is challenging.

SEff and local model properties, such as potential density at each depth horizon and local mean and maximum MLD, had no simple relationship that might suggest a straightforward proxy. A lack of convincing relationship with local properties demonstrates that the downstream pathway of REC is crucial in determining the efficiency of long-term carbon storage.

Defining metrics to capture the spatial variability of REC sequestration depth is challenging as the pathway of remineralized carbon is determined by a combination of the wider circulation, localized physical processes and the depth of the mixed layer downstream of the area where the organic carbon was exported and remineralized. Simple local parameterizations of SEff cannot factor in the subsequent flow pathways and possible re-entrainment of REC, which may lead to future predictions and model estimates of carbon sequestration to be overestimated, particularly if a sequestration horizon of ≤1,000 m is used. A SEff proxy would allow for an improved understanding of the role of and the implications of the future changes in stratification, circulation and biogeochemistry on the predicted magnitude of carbon sequestration.

4.4. Wider Implications of Carbon Sequestration Horizons

The BCP is relevant for climate change mitigation as manipulation or mimicking of the processes that drive the BCP are considered as potential CDR strategies (Gattuso et al., 2021; Siegel et al., 2021). Our findings have implications for CDR and compare well with the findings of Siegel et al. (2021) showing that below 1,000 m, in most regions, dissolved inorganic carbon will be stored for >50 years. However, for some regions, such as the Western North Atlantic, specifically the Gulf stream region, ~70% of exported carbon was transported back to the surface ocean within 50 years (Siegel et al., 2021). Our study also found the Gulf Stream to be an inefficient region for carbon storage, although deep MLD regions were less efficient in our study compared to Siegel et al. (2021). Siegel et al. (2021) found that the North Atlantic and Southern Ocean median sequestration times were shorter compared to the Pacific and Indian Oceans, which highlights the "leaky nature" of some ocean

basins, including the North Atlantic. Ocean CDR methods, such as iron fertilization, can lead to increases in production, but ultimately only a small fraction of the carbon biomass is sequestered on climate-relevant timescales (Siegel et al., 2021). Our study further establishes that oceanic biotic CDR approaches must be able to transfer a large enough magnitude of carbon, usually deeper than the mesopelagic zone, in regions of high SEff to be effective.

Consensus has not been reached as to whether long-term carbon sequestration originating from phytoplankton biomass falls within the Blue Carbon definition (Lovelock & Duarte, 2019). This is due to a lack of scientific understanding of long-term sequestration, possible undesirable anthropogenic impacts, and whether management to reduce greenhouse gas emission is possible, and hence it is not included in current Blue Carbon adaption and mitigation policies (Gattuso et al., 2021; Lovelock & Duarte, 2019). Although, carbon storage via phytoplankton is being considered by other fields of research focusing on assessing the efficiency of CDR approaches (Bach & Boyd, 2021; Siegel et al., 2021). Interestingly, macroalgae exported to the seafloor is considered as an important carbon stock for conservation, management and mitigation and is often included in Blue Carbon assessments, despite undergoing considerable remineralization en route to the seafloor (~75%; Krause-Jensen et al., 2018; Ortega et al., 2019). Oceanic Blue Carbon mitigation strategies require long-term sequestration to be successful and the results of this study highlight regions and depths within the North Atlantic where such strategies may have a higher, or lower, levels of success.

Economic estimates of the value of reducing uncertainty on BCP estimates (Jin et al., 2020) depends heavily on the choice of carbon sequestration horizon. For example, the economic value of scientific research carried out on reducing the uncertainty around estimates of carbon sequestration via the global BCP has been estimated as being on the order of US$0.5 trillion (Jin et al., 2020). The study used a sequestration horizon of 500 m to calculate a lower and upper estimate of CSM and assumes all carbon at 500 m remains sequestered for climate-relevant timescales (Jin et al., 2020). However, CSM estimates at 500 m decreased by 73.6 ± 1.6% once scaled by the centennial SEff presented in this study, which if considered in the Jin et al. (2020) approach may moderate the economic value. This highlights that carbon sequestration by the BCP has a significant economic value and that refining the sequestration horizon depths, and hence the magnitudes of sequestration, has high economic value and is relevant to policy makers (Jin et al., 2020).

Our study also has implications for the reemergence of anthropogenic CO_2 into the mixed layer, which was found to effect the buffering capacity of the upper ocean and may amplify the transient climate sensitivity of the Earth system (Rodgers et al., 2020). Anthropogenic CO_2 has been shown to reemerge into the mixed layer in <10 years in low resolution models (minimum 2° horizontal resolution) and the spatial pattern of positive upward fluxes (obduction) aligns well in the North Atlantic with regions of greater re-entrainment in this study, such as in the Labrador Sea, Gulf stream, North Atlantic Current and North West African Upwelling (Toyama et al., 2017). Our study can provide insights from a higher resolution model of the timescales and locations of reemergence of anthropogenic CO_2 that penetrate to the three depth horizons in the North Atlantic Ocean.

4.5. Advantages and Caveats of the Lagrangian Approach

Offline Lagrangian approaches are utilized due to the reduced computational cost of running simulations and allows for experiments to be designed after the online run, meaning different simulation configurations and criteria can be used. One particular advantage of the parcels package is the ability to extract local model variables along the trajectories. This approach combined with the MLD metric used in this study has the advantage of being coupled with a high-resolution eddy-permitting model and allows for intra- and inter-annual variability in MLD to influence the resulting particle trajectories and sequestration efficiencies, whereas previous studies used temporally static MLD climatologies, often a mean of, or a proxy for, winter MLD (Drake et al., 2018; Robinson et al., 2014). Interannual variability in winter MLD is shown to be important for high latitude ocean ventilation in the North Atlantic in previous Lagrangian simulations, coupled with a similar NEMO-ORCA025 model configuration, with the rate at which water moves away from the subduction region being the critical factor (MacGilchrist et al., 2021). MacGilchrist et al. (2021) also highlights that using a temporally static winter MLD leads to an accumulation of errors when estimating ocean ventilation in the North Atlantic.

The NEMO MLD spatial pattern in the North Atlantic matches well with ARGO-derived MLD observations (Figure 1) although winter MLDs in the Labrador Sea penetrate too deep and too far North (Marzocchi

et al., 2015; Rattan et al., 2010) and in the Greenland, Iceland and Norwegian seas penetrate too deep and extend too far (Figure 1). As our study is model specific we cannot assess the impact of how a shallower temporally variable MLD in the Labrador Sea would alter our findings but using a suite of models in the future could expand on this work, although at a considerable computational cost. As our general findings compare well with independent methods (Siegel et al., 2021; Weber et al., 2016), we do not expect the described differences in MLD to affect our conclusions.

We carried out an MLD sensitivity analysis using a temporally static 20-year average of the annual mean and maximum MLD on a subset of particles (Table S2; Text S1 in Supporting Information S1). The mean re-entrainment timescales of Lagrangian particles were more sensitive to the choice of MLD compared to the SEff but in general, the differences between the different MLD climatologies and the local temporally variable model MLD were small. As expected, using the static mean MLD climatology led to longer median re-entrainment times and greater sequestration efficiencies, whilst the maximum MLD climatology generally led to longer re-entrainment times and lower sequestration efficiencies, but the differences between the latter and the local temporally variable model MLD were negligible (Table S2 and Text S1 in Supporting Information S1).

By using 5 cycles of looped 20-year circulation forcing, our implementation of the Lagrangian approach effectively assumes negligible long-term changes in both the ocean circulation that transports Lagrangian particles and the mixing that ventilates them to the atmosphere. In reality, climate-mediated changes in circulation have already been observed on timescales >20 years, in particular for the Atlantic Meridional Overturning Circulation, a key feature of the ocean's thermohaline circulation in the North Atlantic (DeVries et al., 2017; Menary et al., 2020; Smeed et al., 2018). Similarly, ocean mixing is predicted to generally decline as climate change increases the vertical stratification of the ocean (Capotondi et al., 2012). By decreasing the volume of the ocean that is seasonally mixed, this could increase SEff into the future.

The trajectories are not influenced by mixing or diffusion, both of which are processes that act on dissolved inorganic carbon in the real ocean. We assume here that, below the mixed layer, these two processes should be of lesser importance than the horizontal and vertical velocity components. As we employ an eddy-permitting rather than eddy-resolving model the role of eddies on dissolved carbon distributions in the model will not be fully captured by our Lagrangian approach. More generally, model circulation, mesoscale features and MLDs may vary compared to the real ocean and the results presented here are inevitably model specific. Model resolution may also impact on the particle trajectories and their advective and re-entrainment timescales (Drake et al., 2018), and this is an area that requires further attention. However, our results compare well to other studies using different models and approaches in terms of SEff at different depth horizons (Orr et al., 2001; Siegel et al., 2021).

5. Conclusions

1. Lagrangian analysis shows that North Atlantic Ocean SEff of REC has significant regional variability
2. Assuming a depth horizon of 500 m, 1,000 m and 2,000 m, 28%, 66% and 94% of Lagrangian particles representing REC, respectively was sequestered for a minimum of 100 years, implying long-term storage in the interior ocean
3. The key regions in the North Atlantic Ocean for carbon sequestration are the Subpolar North Atlantic (excluding regions of deep mixing), the Gulf Stream, the North Atlantic Current and the Eastern (sub) tropical North Atlantic
4. Meanwhile, regions of deep winter mixed layers, such as the Labrador Sea, are key regions for re-entrainment of REC into the mixed layer
5. Using our study's SEff maps combined with spatially estimated downward carbon fluxes at 500 m, 1,000 m and 2,000 m finds similar overall sequestration fluxes of 41.3 ± 26.9 TgC yr^{-1} at all depths, with a 74%, 39% and 10% decrease, respectively, from the fixed sequestration horizon estimates that do not account for subsequent ventilation. These results emerge due to the balance between carbon flux attenuation throughout the water column, and SEff increasing with depth
6. Using static and uniform depth horizons across basins may overestimate or underestimate carbon sequestration depending on the region but the cumulative effect is an inflated estimate of North Atlantic CSM

7. No convincing proxy relationships were found to allow carbon SEff to be estimated for low resolution ESMs. This underscores the importance of resolving the downstream pathways of REC for the efficiency of long-term carbon storage
8. These findings have implications for estimates of future predictions of carbon sequestration by global biogeochemical models, which may be overstated, as well as for carbon management strategies, such as oceanic CDR and Blue Carbon schemes, that require long-term sequestration to be successful

Data Availability Statement

The processed Lagrangian output of this study was uploaded to zenodo.org (data set DOIs found in Table S3 in Supporting Information S1) and OceanParcels information and tutorials can be accessed at https://oceanparcels.org/. The underpinning high-resolution Nucleus for European Modeling of the Ocean (NEMO) simulation was performed using the ARCHER UK National Supercomputing Service (https://www.archer2.ac.uk/). The NEMO model output is stored on the JASMIN data analysis environment (https://www.jasmin.ac.uk/).

Acknowledgments
There are no known conflicts of interests for the authors of this study. C.A.B., A.P.M., A.Y. and E.P. were supported by the Natural Environment Research Council (NERC) funding for the CLASS project through grant NE/R015953/1. A.Y. and E.P. were also supported by the NERC National Capability Science Multi-Centre (NCSMC) funding for the UK Earth System Modelling project through grant NE/N018036/1. We would like to acknowledge and thank the Ocean Parcels developers for their efforts. The authors would also like to acknowledge Dr Zoe Jacobs for assistance learning Python, Dr Stephen Kelly for support with the initial experiment design and Professor Stephanie Henson for advice with regard to the estimation of the satellite-derived carbon fluxes. We would like to thank two anonymous reviewers for their constructive reviews and support of the manuscript.

References

Antia, A. N., Von Bodungen, B., & Peinert, R. (1999). Particle flux across the mid-European continental margin. *Deep-Sea Research Part I Oceanographic Research Papers*, *46*(12), 1999–2024. https://doi.org/10.1016/S0967-0637(99)00041-2

Bach, L. T., & Boyd, P. W. (2021). Seeking natural analogs to fast-forward the assessment of marine CO_2 removal. *Proceedings of the National Academy of Sciences*, *118*(40), e2106147118. https://doi.org/10.1073/pnas.2106147118

Behrenfeld, M. J., & Falkowski, P. G. (1997). A consumer's guide to phytoplankton primary productivity models. *Limnology & Oceanography*, *42*(7), 1479–1491. https://doi.org/10.4319/lo.1997.42.7.1479

Blanke, B., & Delecluse, P. (1993). Variability of the tropical Atlantic Ocean simulated by a general circulation model with two different mixed-layer physics. *Journal of Physical Oceanography*, *23*(7), 1363–1388. https://doi.org/10.1175/1520-0485(1993)023<1363:VOTTAO>2.0.CO;2

Bopp, L., Monfray, P., Aumont, O., Dufresne, J. L., Le Treut, H., Madec, G., et al. (2001). Potential impact of climate change on marine export production. *Global Biogeochemical Cycles*, *15*(1), 81–99. https://doi.org/10.1029/1999GB001256

Bouillon, S., Morales Maqueda, M. Á., Legat, V., & Fichefet, T. (2009). An elastic-viscous-plastic sea ice model formulated on Arakawa B and C grids. *Ocean Modelling*, *27*(3–4), 174–184. https://doi.org/10.1016/j.ocemod.2009.01.004

Bower, A., Lozier, S., Biastoch, A., Drouin, K., Foukal, N., Furey, H., et al. (2019). Lagrangian views of the pathways of the Atlantic meridional overturning circulation. *Journal of Geophysical Research: Oceans*, *124*(8), 5313–5335. https://doi.org/10.1029/2019JC015014

Boyd, P. W., Claustre, H., Levy, M., Siegel, D. A., & Weber, T. (2019). Multi-faceted particle pumps drive carbon sequestration in the ocean. *Nature*, *568*(7752), 327–335. https://doi.org/10.1038/s41586-019-1098-2

Boyd, P. W., & Trull, T. W. (2007). Understanding the export of biogenic particles in oceanic waters: Is there consensus? *Progress in Oceanography*, *72*(4), 276–312. https://doi.org/10.1016/j.pocean.2006.10.007

Briggs, N., Perry, M. J., Cetinić, I., Lee, C., D'Asaro, E., Gray, A. M., & Rehm, E. (2011). High-resolution observations of aggregate flux during a sub-polar North Atlantic spring bloom. *Deep-Sea Research Part I Oceanographic Research Papers*, *58*(10), 1031–1039. https://doi.org/10.1016/j.dsr.2011.07.007

Brodeau, L., Barnier, B., Treguier, A. M., Penduff, T., & Gulev, S. (2010). An ERA40-based atmospheric forcing for global ocean circulation models. *Ocean Modelling*, *31*(3–4), 88–104. https://doi.org/10.1016/j.ocemod.2009.10.005

Cael, B. B., & Bisson, K. (2018). Particle flux parameterizations: Quantitative and mechanistic similarities and differences. *Frontiers in Marine Science*, *5*, 1–5. https://doi.org/10.3389/fmars.2018.00395

Capotondi, A., Alexander, M. A., Bond, N. A., Curchitser, E. N., & Scott, J. D. (2012). Enhanced upper ocean stratification with climate change in the CMIP3 models. *Journal of Geophysical Research*, *117*(C4), C04031. https://doi.org/10.1029/2011JC007409

Carr, M. E. (2002). Estimation of potential productivity in Eastern Boundary Currents using remote sensing. *Deep-Sea Research Part II Topical Studies in Oceanography*, *49*(1–3), 59–80. https://doi.org/10.1016/S0967-0645(01)00094-7

de Boyer Montégut, C., Madec, G., Fischer, A. S., Lazar, A., & Iudicone, D. (2004). Mixed layer depth over the global ocean: An examination of profile data and a profile-based climatology. *Journal of Geophysical Research - C: Oceans*, *109*(12), 1–20. https://doi.org/10.1029/2004JC002378

Delandmeter, P., & Van Sebille, E. (2019). The Parcels v2.0 Lagrangian framework: New field interpolation schemes. *Geoscientific Model Development*, *12*(8), 3571–3584. https://doi.org/10.5194/gmd-12-3571-2019

Devries, T. (2014). The oceanic anthropogenic CO_2 sink: Storage, air-sea fluxes, and transports over the industrial era. *Global Biogeochemical Cycles*, *28*(7), 631–647. https://doi.org/10.1002/2013GB004739

DeVries, T., Holzer, M., & Primeau, F. (2017). Recent increase in oceanic carbon uptake driven by weaker upper-ocean overturning. *Nature*, *542*(7640), 215–218. https://doi.org/10.1038/nature21068

DeVries, T., & Primeau, F. (2011). Dynamically and observationally constrained estimates of water-mass distributions and ages in the global ocean. *Journal of Physical Oceanography*, *41*(12), 2381–2401. https://doi.org/10.1175/JPO-D-10-05011.1

DeVries, T., Primeau, F., & Deutsch, C. (2012). The sequestration efficiency of the biological pump. *Geophysical Research Letters*, *39*(13), 1–5. https://doi.org/10.1029/2012GL051963

Drake, H. F., Morrison, A. K., Griffies, S. M., Sarmiento, J. L., Weijer, W., & Gray, A. R. (2018). Lagrangian timescales of Southern Ocean upwelling in a hierarchy of model resolutions. *Geophysical Research Letters*, *45*(2), 891–898. https://doi.org/10.1002/2017GL076045

Dunne, J. P., Sarmiento, J. L., & Gnanadesikan, A. (2007). A synthesis of global particle export from the surface ocean and cycling through the ocean interior and on the seafloor. *Global Biogeochemical Cycles*, *21*(4), 1–16. https://doi.org/10.1029/2006GB002907

Gattuso, J.-P., Williamson, P., Duarte, C. M., & Magnan, A. K. (2021). The potential for ocean-based climate action: Negative emissions technologies and beyond. *Frontiers in Climate*, *2*(January), 1–8. https://doi.org/10.3389/fclim.2020.575716

Gent, P. R., & Mcwilliams, J. C. (1990). Isopycnal mixing in ocean circulation models. *Journal of Physical Oceanography*, *20*(1), 150–155. https://doi.org/10.1175/1520-0485(1990)020<0150:IMIOCM>2.0.CO;2

Georgiou, S., Ypma, S. L., Brüggemann, N., Sayol, J. M., Pietrzak, J. D., & Katsman, C. A. (2020). Pathways of the water masses exiting the Labrador Sea: The importance of boundary–interior exchanges. *Ocean Modelling*, *150*(November 2019), 101623. https://doi.org/10.1016/j.ocemod.2020.101623

Guidi, L., Legendre, L., Reygondeau, G., Uitz, J., Stemmann, L., & Henson, S. A. (2015). A new look at ocean carbon remineralization for estimating deepwater sequestration. *Global Biogeochemical Cycles*, *29*(7), 1044–1059. https://doi.org/10.1002/2014GB005063

Helmke, P., Romero, O., & Fischer, G. (2005). Northwest African upwelling and its effect on offshore organic carbon export to the deep sea. *Global Biogeochemical Cycles*, *19*(4), 1–16. https://doi.org/10.1029/2004GB002265

Henson, S. A., Sanders, R., & Madsen, E. (2012). Global patterns in efficiency of particulate organic carbon export and transfer to the deep ocean. *Global Biogeochemical Cycles*, *26*(1), 1–14. https://doi.org/10.1029/2011GB004099

Henson, S. A., Sanders, R., Madsen, E., Morris, P. J., Le Moigne, F., & Quartly, G. D. (2011). A reduced estimate of the strength of the ocean's biological carbon pump. *Geophysical Research Letters*, *38*(4). https://doi.org/10.1029/2011GL046735

Herzog, H., Caldeira, K., Reilly, J., Jacoby, H. D., & Prinn, R. G. (2002). *An issue of permanence: Assessing the effectiveness of temporary carbon storage*.

Heuzé, C. (2017). North Atlantic deep water formation and AMOC in CMIP5 models. *Ocean Science Discussions*, 1–22. https://doi.org/10.5194/os-2017-2

Holte, J., Talley, L. D., Gilson, J., & Roemmich, D. (2017). An Argo mixed layer climatology and database. *Geophysical Research Letters*, *44*(11), 5618–5626. https://doi.org/10.1002/2017GL073426

IPCC. (2007). *Climate change 2007 synthesis report. Intergovernmental Panel on climate change core writing team IPCC*. https://doi.org/10.1256/004316502320517344

Ito, T., & Follows, M. J. (2013). Air-sea disequilibrium of carbon dioxide enhances the biological carbon sequestration in the Southern Ocean. *Global Biogeochemical Cycles*, *27*(4), 1129–1138. https://doi.org/10.1002/2013GB004682

Jin, D., Hoagland, P., & Buesseler, K. O. (2020). The value of scientific research on the ocean's biological carbon pump. *The Science of the Total Environment*, *749*, 141357. https://doi.org/10.1016/j.scitotenv.2020.141357

Jones, D. C., Ito, T., Takano, Y., & Hsu, W. C. (2014). Spatial and seasonal variability of the air-sea equilibration timescale of carbon dioxide. *Global Biogeochemical Cycles*, *28*(11), 1163–1178. https://doi.org/10.1002/2014GB004813

Kounta, L., Capet, X., Jouanno, J., Kolodziejczyk, N., Sow, B., & Thierno Gaye, A. (2018). A model perspective on the dynamics of the shadow zone of the eastern tropical North Atlantic-Part 1: The poleward slope currents along West Africa. *Ocean Science*, *14*(5), 971–997. https://doi.org/10.5194/os-14-971-2018

Krause-Jensen, D., Lavery, P., Serrano, O., Marba, N., Masque, P., & Duarte, C. M. (2018). Sequestration of macroalgal carbon: The elephant in the Blue Carbon room. *Biology Letters*, *14*(6). https://doi.org/10.1098/rsbl.2018.0236

Kwon, E. Y., Primeau, F., & Sarmiento, J. L. (2009). The impact of remineralization depth on the air–sea carbon balance. *Nature Geoscience*, *2*(9), 630–635. https://doi.org/10.1038/ngeo612

Lampitt, R., Achterberg, E., Anderson, T., Hughes, J., Iglesias-Rodriguez, M., Kelly-Gerreyn, B., et al. (2008). Ocean fertilization: A potential means of geoengineering? *Philosophical Transactions of the Royal Society A: Mathematical, Physical & Engineering Sciences*, *366*(1882), 3919–3945. https://doi.org/10.1098/rsta.2008.0139

Lampitt, R. S., Salter, I., de Cuevas, B. A., Hartman, S., Larkin, K. E., & Pebody, C. A. (2010). Long-term variability of downward particle flux in the deep northeast Atlantic: Causes and trends. *Deep Sea Research Part II: Topical Studies in Oceanography*, *57*(15), 1346–1361. https://doi.org/10.1016/j.dsr2.2010.01.011

Lange, M., & Van Sebille, E. (2017). Parcels v0.9: Prototyping a Lagrangian ocean analysis framework for the petascale age. *Geoscientific Model Development*, *10*(11), 4175–4186. https://doi.org/10.5194/gmd-10-4175-2017

Liu, M., & Tanhua, T. (2021). Water masses in the Atlantic Ocean: Characteristics and distributions. *Ocean Science*, *17*(2), 463–486. https://doi.org/10.5194/os-17-463-2021

Lovelock, C. E., & Duarte, C. M. (2019). Dimensions of blue carbon and emerging perspectives. *Biology Letters*, *15*(3), 1–5. https://doi.org/10.1098/rsbl.2018.0781

Lutz, M., Dunbar, R., & Caldeira, K. (2002). Regional variability in the vertical flux of particulate organic carbon in the ocean interior. *Global Biogeochemical Cycles*, *16*(3). https://doi.org/10.1029/2000GB001383

Lutz, M. J., Caldeira, K., Dunbar, R. B., & Behrenfeld, M. J. (2007). Seasonal rhythms of net primary production and particulate organic carbon flux to depth describe the efficiency of biological pump in the global ocean. *Journal of Geophysical Research*, *112*(C10), C10011. https://doi.org/10.1029/2006JC003706

Luyten, J. R., Pedlosky, J., & Stommel, H. (1983). The ventilated thermocline. *Journal of Physical Oceanography*, *13*(2), 292–309. https://doi.org/10.1175/1520-0485(1983)013<0292:TVT>2.0.CO;2

MacGilchrist, G. A., Johnson, H. L., Lique, C., & Marshall, D. P. (2021). Demons in the North Atlantic: Variability of deep ocean ventilation. *Geophysical Research Letters*, *48*(9), 1–9. https://doi.org/10.1029/2020GL092340

Madec, G. (2014). NEMO ocean engine, (27).

Marcello, J., Hernández-Guerra, A., Eugenio, F., & Fonte, A. (2011). Seasonal and temporal study of the northwest African upwelling system. *International Journal of Remote Sensing*, *32*(7), 1843–1859. https://doi.org/10.1080/01431161003631576

Martin, J. H., Knauer, G. A., Karl, D. M., & Broenkow, W. W. (1987). Vertex: Carbon cycling in the northeast Pacific. *Deep-Sea Research Part A. Oceanographic Research Papers*, *34*(2), 267–285. https://doi.org/10.1016/0198-0149(87)90086-0

Martin, P., Lampitt, R. S., Jane Perry, M., Sanders, R., Lee, C., & D'Asaro, E. (2011). Export and mesopelagic particle flux during a North Atlantic spring diatom bloom. *Deep-Sea Research Part I Oceanographic Research Papers*, *58*(4), 338–349. https://doi.org/10.1016/j.dsr.2011.01.006

Marzocchi, A., Hirschi, J. J. M., Holliday, N. P., Cunningham, S. A., Blaker, A. T., & Coward, A. C. (2015). The North Atlantic subpolar circulation in an eddy-resolving global ocean model. *Journal of Marine Systems*, *142*, 126–143. https://doi.org/10.1016/j.jmarsys.2014.10.007

Marzocchi, A., Nurser, A. J. G., Clément, L., & McDonagh, E. (2021). Surface atmospheric forcing as the driver of long-term pathways and timescales of ocean ventilation. *Ocean Science Discussions*, 1–27. https://doi.org/10.5194/os-2021-4

Menary, M. B., Robson, J., Allan, R. P., Booth, B. B. B., Cassou, C., Gastineau, G., et al. (2020). Aerosol-forced AMOC changes in CMIP6 historical simulations. *Geophysical Research Letters*, *47*(14). https://doi.org/10.1029/2020GL088166

Mittelstaedt, E. (1983). The upwelling area off Northwest Africa-A description of phenomena related to coastal upwelling. *Progress in Oceanography*, *12*(3), 307–331. https://doi.org/10.1016/0079-6611(83)90012-5

Mittelstaedt, E. (1991). The ocean boundary along the northwest African coast: Circulation and oceanographic properties at the sea surface. *Progress in Oceanography*, *26*(4), 307–355. https://doi.org/10.1016/0079-6611(91)90011-A

Orr, J. C., Aumont, O., Yool, A., Plattner, K., Joos, F., Maier-Reimer, E., et al. (2001). Ocean CO_2 sequestration efficiency from 3-D ocean model comparison. *Proceedings of the Fifth Int. Conf. on Greenhouse Gas Control Technologies*, 469–474.

Ortega, A., Geraldi, N. R., Alam, I., Kamau, A. A., Acinas, S. G., Logares, R., et al. (2019). Important contribution of macroalgae to oceanic carbon sequestration. *Nature Geoscience*, *12*(9), 748–754. https://doi.org/10.1038/s41561-019-0421-8

Pabortsava, K., Lampitt, R. S., Benson, J., Crowe, C., McLachlan, R., Le Moigne, F. A. C., et al. (2017). Carbon sequestration in the deep Atlantic enhanced by Saharan dust. *Nature Geoscience*, *10*(3), 189–194. https://doi.org/10.1038/ngeo2899

Palevsky, H. I., & Doney, S. C. (2021). Sensitivity of 21st century ocean carbon export flux projections to the choice of export depth horizon. *Global Biogeochemical Cycles*, *35*(2), 1–24. https://doi.org/10.1029/2020gb006790

Passow, U., & Carlson, C. (2012). The biological pump in a high CO_2 world. *Marine Ecology Progress Series*, *470*(2), 249–271. https://doi.org/10.3354/meps09985

Pickart, R. S., Torres, D. J., & Clarke, R. A. (2002). Hydrography of the Labrador Sea during active convection. *Journal of Physical Oceanography*, *32*(2), 428–457. https://doi.org/10.1175/1520-0485(2002)032<0428:HOTLSD>2.0.CO;2

Primeau, F. (2005). Characterizing transport between the surface mixed layer and the ocean interior with a forward and adjoint global ocean transport model. *Journal of Physical Oceanography*, *35*(4), 545–564. https://doi.org/10.1175/JPO2699.1

Quay, P., Stutsman, J., & Steinhoff, T. (2012). Primary production and carbon export rates across the subpolar N. Atlantic Ocean basin based on triple oxygen isotope and dissolved O_2 and Ar gas measurements. *Global Biogeochemical Cycles*, *26*(2). https://doi.org/10.1029/2010GB004003

Rattan, S., Myers, P. G., Treguier, A. M., Theetten, S., Biastoch, A., & Böning, C. (2010). Towards an understanding of Labrador Sea salinity drift in eddy-permitting simulations. *Ocean Modelling*, *35*(1–2), 77–88. https://doi.org/10.1016/j.ocemod.2010.06.007

Robinson, J., Popova, E. E., Yool, A., Srokosz, M., Lampitt, R. S., & Blundell, J. R. (2014). How deep is deep enough? Ocean iron fertilization and carbon sequestration in the Southern Ocean. *Geophysical Research Letters*, *41*(7), 2489–2495. https://doi.org/10.1002/2013GL058799

Rodgers, K. B., Schlunegger, S., Slater, R. D., Ishii, M., Frölicher, T. L., Toyama, K., et al. (2020). Reemergence of anthropogenic carbon into the ocean's mixed layer strongly amplifies transient climate sensitivity. *Geophysical Research Letters*, *47*(18), 1–9. https://doi.org/10.1029/2020GL089275

Sanders, R., Henson, S. A., Koski, M., De La Rocha, C. L., Painter, S. C., Poulton, A. J., et al. (2014). The biological carbon pump in the North Atlantic. *Progress in Oceanography*, *129*, 200–218. https://doi.org/10.1016/j.pocean.2014.05.005

Santos, I. R., Burdige, D. J., Jennerjahn, T. C., Bouillon, S., Cabral, A., Serrano, O., et al. (2021). The renaissance of Odum's outwelling hypothesis in "Blue Carbon" science. *Estuarine, Coastal and Shelf Science*, *255*(December 2020), 107361. https://doi.org/10.1016/j.ecss.2021.107361

Siegel, D. A., DeVries, T., Doney, S. C., & Bell, T. (2021). Assessing the sequestration time scales of some ocean-based carbon dioxide reduction strategies. *Environmental Research Letters*. https://doi.org/10.1016/j.snb.2007.07.003

Smeed, D. A., Josey, S. A., Beaulieu, C., Johns, W. E., Moat, B. I., Frajka-Williams, E., et al. (2018). The North Atlantic Ocean is in a state of reduced overturning. *Geophysical Research Letters*, *45*(3), 1527–1533. https://doi.org/10.1002/2017GL076350

Steinacher, M., Joos, F., Frölicher, T. L., Bopp, L., Cadule, P., Cocco, V., et al. (2010). Projected 21st century decrease in marine productivity: A multi-model analysis. *Biogeosciences*, *7*(3), 979–1005. https://doi.org/10.5194/bg-7-979-2010

Tamsitt, V., Drake, H. F., Morrison, A. K., Talley, L. D., Dufour, C. O., Gray, A. R., et al. (2017). Spiraling pathways of global deep waters to the surface of the Southern Ocean. *Nature Communications*, *8*(1), 1–10. https://doi.org/10.1038/s41467-017-00197-0

Toyama, K., Rodgers, K. B., Blanke, B., Iudicone, D., Ishii, M., Aumont, O., & Sarmiento, J. L. (2017). Large reemergence of anthropogenic carbon into the ocean's surface mixed layer sustained by the ocean's overturning circulation. *Journal of Climate*, *30*(21), 8615–8631. https://doi.org/10.1175/JCLI-D-16-0725.1

van Sebille, E., Griffies, S. M., Abernathey, R., Adams, T. P., Berloff, P., Biastoch, A., et al. (2018). Lagrangian ocean analysis: Fundamentals and practices. *Ocean Modelling*, *121*(October 2017), 49–75. https://doi.org/10.1016/j.ocemod.2017.11.008

Volk, T., & Hoffert, M. I. (1985). Ocean carbon pumps: Analysis of relative strengths and efficiencies in ocean-driven atmospheric CO_2 changes. In *The carbon cycle and atmospheric CO_2: Natural variations Archean to present* (Vol. 32, pp. 99–110). American Geophysical Union. https://doi.org/10.1029/GM032p0099

Weber, T., Cram, J. A., Leung, S. W., DeVries, T., & Deutsch, C. (2016). Deep ocean nutrients imply large latitudinal variation in particle transfer efficiency. *Proceedings of the National Academy of Sciences*, *113*(31), 8606–8611. https://doi.org/10.1073/pnas.1604414113

Yashayaev, I., & Clarke, A. (2008). Evolution of North Atlantic water masses inferred from Labrador Sea salinity series. *Oceanography*, *21*(1), 30–45. https://doi.org/10.5670/oceanog.2008.65

Yool, A., Popova, E. E., & Anderson, T. R. (2013). MEDUSA-2.0: An intermediate complexity biogeochemical model of the marine carbon cycle for climate change and ocean acidification studies. *Geoscientific Model Development*, *6*(5), 1767–1811. https://doi.org/10.5194/gmd-6-1767-2013

Yool, A., Popova, E. E., & Coward, A. C. (2015). Future change in ocean productivity: Is the Arctic the new Atlantic? *Geophysical Research*, *120*(12), 7771–7790. https://doi.org/10.1002/2015JC011167